63-2-4

ASD TECHNICAL REPORT 61-253

CRYSTAL RATE GYRO

Lloyd Germain
Thomas Wing

GULTON INDUSTRIES, INC.
Metuchen, New Jersey

Contract No. AF33(616)-5561

AUGUST 1961

NAVIGATION AND GUIDANCE LABORATORY
AERONAUTICAL SYSTEMS DIVISION
AIR FORCE SYSTEMS COMMAND
UNITED STATES AIR FORCE

WRIGHT-PATTERSON AIR FORCE BASE, OHIO

NOTICES

When Government drawings, specifications, or other data are used for any purpose other than in connection with a definitely related Government procurement operation, the United States Government thereby incurs no responsibility nor any obligation whatsoever; and the fact that the Government may have formulated, furnished, or in any way supplied the said drawings, specifications, or other data, is not to be regarded by implication or otherwise as in any manner licensing the holder or any other person or corporation, or conveying any rights or permission to manufacture, use, or sell any patented invention that may in any way be related thereto.

*

Qualified requesters may obtain copies of this report from the Armed Services Technical Information Agency, (ASTIA), Arlington Hall Station, Arlington 12, Virginia.

*

Copies of ASD Technical Reports and Technical Notes should not be returned to the Aeronautical Systems Division unless return is required by security considerations, contractual obligations, or notice on a specific document.

ASD TECHNICAL REPORT 61-253

CRYSTAL RATE GYRO

Lloyd Germain and Thomas Wing

GULTON INDUSTRIES, INC.

AUGUST 1961

NAVIGATION AND GUIDANCE LABORATORY

CONTRACT NO. AF33(616)-5561
PROJECT NO. 0(610-4431)
TASK NO. 50758

AERONAUTICAL SYSTEMS DIVISION
AIR FORCE SYSTEMS COMMAND
UNITED STATES AIR FORCE
WRIGHT-PATTERSON AIR FORCE BASE, OHIO

FOREWORD

This report was prepared by the Research and Development Laboratory of Gulton Industries, Inc. on U. S. Air Force Contract No. AF33(616)-5561, under Task No. 50758 of Project No. 0(610-4431), "Crystal Rate Gyro." The work was administered under the direction of the Navigation and Guidance Laboratory, Aeronautical Systems Division. Captain James E. Stephens was task engineer for the laboratory.

This report covers work conducted from March 1958 to March 1961.

The assistance of Robert TenEyck is gratefully acknowledged, and special acknowledgment is given to Daniel S. Schwartz and Dr. Irving Bogner for their work in the earlier portion of this contract. The cooperation of the Bendix Corporation at Teterboro, New Jersey for the generous use of their gyro test equipment is gratefully acknowledged.

This report concludes the work on Contract AF33(616)-5561.

ABSTRACT

This report is concerned with efforts by Gulton Industries to fabricate a vibratory gyro to detect very low rates of turn. The field of endeavor fell into three phases. Phase I dealt with attempts to utilize piezo-electric ceramics as the vibratory element. Various configurations and measurements are discussed in detail. The maximum output was 500 μv at 360°/sec with a zero rate of 3800 μv without repeatability. Phase II was concerned with the use of lower frequency electro-meahcnical vibratory elements in measuring the required angular rates. The results obtained from using the resultant crude tuning forks rate sensors are fully discussed. Using null circuitry at 0.5 rpm, an output of 2 volts was obtained for signal to noise ratio of 1. This was not repeatable without readjustment. Although far from satisfactory, the results of Phase II indicated the correct direction to continue. Phase III dealt with fabrications of precision tuning forks. The results achieved are discussed and solutions to problems are proposed. Under optimum conditions, the refined gyro was able to detect a rate of 1 revolution in 100 days.

TABLE OF CONTENTS

TABLE OF CONTENTS - Continued

TABLE OF CONTENTS - Continued

LIST OF ILLUSTRATIONS

INTRODUCTION

On March 15, 1958, the Research and Development Laboratories of Gulton Industries, Inc. began a continuing research and development program to investigate the possibilities of the crystal rate gyroscope. The program consisted of three distinct phases, each lasting approximately one year. Phase I was actually a continuation of the work performed by Goodyear and Clevite, during which the possibilities of a crystal rate gyro based on a vibratory piezoelectric member (inertial disc) were investigated. Phase II consisted in the main of a re-evaluation program which led to low frequency - high amplitude vibrators such as the tuning fork. Phase III was a period devoted to refinement of the tuning fork gyro, both mechanically and electronically. The ultimate aim of the program was to develop a vibratory gyro which had high sensitivity, small size, long life, and was low in cost and power consumption.

This report summarizes in detail the results of a three-year effort to meet the goals set. The resultant gyro is a precision tuning fork design which is capable of detecting angular rates on the order of 1 revolution in 180 days, under optimum conditions.

Manuscript released by authors August 1961 for publication as an ASD Technical Report.

1. PHASE I

1.1 SCOPE

The program for Phase I covered the study and development of a rate gyroscope based on a vibrating piezoelectric member. The objective was to obtain an improved angular rate sensor capable of extreme sensitivity, high accuracy, and which would be more compact in design, and lower in production cost than present rotary types. The program included a study and investigation period followed by construction of an experimental gyro to demonstrate feasibility. Conformance to the standards of MIL-E-5400 was not within the scope of this project.

On the basis of studies made prior to this work, the ultimate target objective was to develop a device having a threshold sensitivity of 0.005 degrees per hour and a maximum size of 3 inches in any dimension. It should be noted that the desired sensitivity is considerably beyond that attainable in any presently available commercial gyro.

1.2 INITIAL STUDIES

A review of existing work on vibratory gyros and a subsequent critical examination of attempted crystal rate gyro configurations were undertaken in an attempt to extract all pertinent data available concerning this project. It was thought that a detailed critical analysis of previous work would be of value, but an examination of Table 1 clearly indicated that this would be unnecessary. Completely new approaches had to be utilized in order to attain the desired sensitivity of the contemplated gyro.

Table 1 is a compilation of results obtained by Goodyear (References 1 and 2) and the Clevite group (Reference 3). Note that the residual output at zero rate of turn is somewhat of a noise or unwanted figure. The ratio

$$\frac{\text{sensitivity (mv/°/sec.)}}{\text{zero turn output (mv)}}$$

is a modified signal-to-noise ratio and is much less than 1 for every case. These are listed here as the reciprocal of the above ratio. The high frequency type ring and cylinder had a noise-to-signal ratio of 40×10^3 and possessed extremely poor stability. It was apparent that if the target sensitivity (1.39×10^{-6}°/sec) was used in the above ratio, these configurations are too low in sensitivity by large orders of magnitude. Although it might have been possible to further refine these configurations and obtain better results, emphasis was placed on new approaches. The first new approaches contemplated are briefly outlined below.

1.2.1 Wagon Wheel Configuration

The basic structure of the wagon wheel design consists of two discs, which vibrate in opposite directions as a result of polarizing and phasing, separated and supported by a group of flat ceramic bender pickup elements similar to phonograph pickups. These pickups are attached to the discs in such a manner that their bending sensitive direction is tangent to the circumference of the discs. The combination of pickup elements in series electrically will give a high output voltage while the combination of elements mechanically in parallel will increase the resonant frequency with number. It was shown (Reference 4) that a 3 disc, 20 bender element system might detect an angular rate of 1.6×10^{-4} degrees/sec. under optimum conditions.

1.2.2 Axle Configurations

The torque produced by the vibrating member depends upon the mass of the material, the amplitude of radial vibration, the impressed rate of turn, and the velocity distribution within the member. The simplest shape from the points of view of fabrication and calculation is a round disc whose radial resonant frequency is primarily a function of diameter. Using a piezoelectric ceramic, the radial vibrations may be excited by electroding the flat faces, polarizing in thickness, and applying drive voltage across the thickness. However, this method depends on cross coupling between radial and axial modes and suffers a consequent loss. Direct drive could be accomplished by boring out the center of the disc, electroding within the hole and along the circumference, and polarizing radially. The increased efficiency in terms of greater radial displacement for a given drive voltage, the frequency being the same as in the above case, should result in higher velocities and hence, greater sensitivity to turn rate. The mass removed at the center is a small portion of the whole and lies in a region of minimum velocity (centered about the node). To increase the mass, and thus the rate of change of angular momentum (or torque), the disc should be thick. However, the radial resonant frequency should be the lowest for all modes to prevent cross-coupling (which would result in a loss of radial drive energy). The minimal loss of mass due to boring has little effect on the radial resonant frequency.

To sense rotation, the vibrating disc must be rigidly connected to some structure which orients the disc relative to the axis of rotation. In a previous attempt, the disc was bonded to a torsion pickup in the form of a cylinder, the axis of which was also the axis of rotation. This pickup cylinder must have a high mechanical Q and be tuned to have a torsional resonant frequency equal to that of the radial resonant frequency of the disc to give a significant output, a most difficult goal. Ideally, the mechanical connection should be made at a node to minimize the effects of cross-coupling to the vertical mode. The axial configurations are designed to utilize this precept.

1.2.2.1 Axle Bender Design

In the axle bender design, a metallic axle is cemented to the disc through a hole at its center (node). Conducting cement was contemplated; however, soldering may be required. The axle and disc assembly is suspended coaxially in a tube by thin ceramic bender elements cemented to the axle and tube. Rotation of the tube will cause an output from the ceramic bender elements which are electrically series-connected.

1.2.2.2 Pin Wheel Design

In the pin wheel configuration, the metal axle and disc assembly is similar to the axle bender design. At the ends of the axle, which is the axis of rotation and acts as the torsion transmitting member, are metal pinwheels which are supported by and bonded to piezoelectric ceramic rods. These rods are bonded to a rigid framework. Torque, impressed on the axle, causes compression or tension against the ceramic rods and produces the output. The axle must have high mechanical Q and be tuned to the radial resonant frequency of the disc as in the previous design. Direction of rotation is determined by comparing the phase of the output to that of the driving voltage.

1.2.3 Crystal Rate Gyro Materials

Prior to this work, a reasonable amount of effort had been expended on the theoretical analysis of the crystal rate gyro and its possibilities. The main limitation of these works had been the paucity of reliable data. The objective of these preliminary studies was then to extract basic design parameters from which accurate predictions of performance possibilities could be obtained and applied to a given design or configuration.

The crystal rate gyro consists of the following basic parts:

(1) Piezoelectric ceramic inertial member

(2) Torque summing members

(3) Oscillator and driving system

(4) Appropriate circuitry for processing the output signal.

Of these four, items (3) and (4) required little initial study, being somewhat routine. Thus, the bulk of effort was applied to items (1) and (2). The special parameters associated with these parts cannot be obtained theoretically or required empirical confirmation. These included the following:

(1) Measurement of the torsional amplitude of the inertial member at varying speeds and varying excitations.

(2) Evaluation of pickoff devices.

(3) The effect of loading by the pickoff device on the driving member.

Of primary importance to the satisfactory performance of the crystal rate gyro were the properties of the piezoelectric ceramic. The ceramic material had to be stable, exhibiting negligible drift with time and environment or be rendered worthless. Thus, effort was concentrated on the following techniques and properties of proposed ceramic materials.

(1) Optimum poling techniques for piezoelectric ceramics.

(2) Physical, electrical, and electromechanical properties of various ceramic fabrications.

(3) Piezoelectric sensitivity and resonant frequency stability with time after poling.

(4) Response after long and short term storage at various temperatures.

(5) Piezoelectric output and efficiencies after various times of operation in various modes of motion.

1.2.3.1 HT-14 Ceramics

HT-14, a lead titanate - lead zirconate body manufactured by Gulton Industries, was first considered on the bases of its high Curie point (350 - 400°C) and expected superior performance at room temperatures. Samples of this material were divided into five groups and subjected to storage at +165°F, room temperature, -65°F, and high and low temperature cycling over various periods from one week to eight months. The long period data was abstracted from previous Gulton work. Capacitance values were recorded before and after poling and after the test periods. In addition, variations in dissipation factor, insulation resistance, and low force d_{33} sensitivity were noted. The conclusions derived from these tests were as follows:

(1) Neither high, low, nor mixed temperature cycling had any great effect on the dissipation factor or insulation resistance.

(2) If the HT-14 samples are separated into relatively high or low initial capacitance or relative dielectric constant groups, then:

(a) Cold cycling, to -50°C, had little effect on the low capacitance group while the relatively high capacitance

group should be reprocessed or discarded as being unstable or possessing undesirable capacitance and sensitivity aging characteristics.

(b) Hot cycling, to +74°C, had little effect on the low capacitance group but introduced capacitance and sensitivity instability in the high capacitance group.

(c) Samples with relatively low capacitance appear to be much less subject to capacitance and sensitivity variations due to mixed temperature cycling than the high capacitance group.

(3) Mixed temperature cycling during polarization would lead to better aging characteristics with time after poling and also to better uniformity in dielectric constant.

1.2.3.2 Body 103 Ceramics

After full consideration of pros and cons regarding types of ceramics for the initial work, low temperature Body 103 ceramics were selected, mostly for cost and ease of fabrication. Much reliable data was available for this material and cut test times appreciably.

1.2.4 Pickoff Devices

Consideration was given to non-loading pickoff devices, such as optical and capacitive types, in the event the proposed piezoelectric ceramic types proved unsatisfactory.

Work on ceramic pickoffs centered around the use of warped ceramic sensors as suggested previously (reference 4). It was determined in previous work at Gulton that apparent d_{33} values on the order of 35 times higher could be obtained by the use of warped ceramic elements. Some conclusions drawn from these tests were as follows:

(1) High sensitivity diminishes with preload. Thus the large output (compared to the true d_{33} coefficient) could only be utilized at low forces unless more ceramic distortion is used.

(2) No great change of sensitivity is evident with aging after polarization.

(3) If the samples were intentionally cut in the shape of a section of a sphere, ellipsoid, hyperboloid, or other solid of revolution, this high output might be extended to higher forces. Thus a stress in a compressional mode might be

made to give compressional, bending, and torsional mode charge releases.

(4) Similar high output results were obtained using an extremely poor polarization. This proves conclusively that the high output obtained is not due to polarization techniques but to shape factors of the ceramics.

(5) As expected, some of the highly warped ceramic samples cracked as a result of first loading. This indicated the need for more work on the structural strength of these members.

(6) One of the samples tested, which was much less warped than the other samples, gave much less output than the warped samples. Thus the high output noted can definitely be ascribed to modes other than the compressional d_{33} modes.

1.3 VIBRATORY DISPLACEMENT MEASUREMENT

Information regarding location of nodes or nodal regions was of great interest, as well as the correlation between drive potential and vibratory displacements for the ceramic disc configurations. Methods for attaining these ends were conceived and executed.

The samples used in these tests were solid ceramic discs, i.e., no attempt was made to drive the disc radially at this time. The discs were face polarized and face electroded and radial excitation was effected through cross-coupling of thickness and radial modes, despite an expectedly large loss in driving energy. These discs were mounted by pins at the center or nodal region to minimize transmitted losses. Information on d_{31}, the piezoelectric modulus for this mode of excitation, was necessary, and theoretical and experimental values were determined.

1.3.1 Microscopic Study

A Unitron metallurgical microscope was obtained for a first attempt to probe the disc optically for nodes and vibration amplitudes. This instrument was capable, using a 4 : 1 interpolation of the fine division, of noting vibration amplitudes of 25 microinches. Notation of amplitudes under driving forces on the order of 800 volts should be detected. A theoretical calculation, assuming a mechanical Q of 100, for a given sample was on the order of 200 microinches.

Upon prolonged operation at 50V rms, however, the sample ceramic became exceedingly hot. For this Body 103 ceramic, operation above 80°C causes irreversible pyroelectric effects which result in permanent loss of sensitivity upon cooling. It was later determined that 50 volts was a

maximum value for this material. Deflections at this potential were so small as to render the use of microscopic techniques unsatisfactory. The high temperature noted was not a serious drawback since the proposed HT-14 ceramic has a Curie point $\cong$ 375°C.

1.3.2 Temperature Tests

Because of the effect noted above, two simple experiments were conducted to determine the relationship between peak driving voltage and surface temperature, and the effects of temperature change on resonant frequency. It was important that these inter-relationships be established fairly early in the program since driving the ceramic too hard may be expected to tend to depole the ceramic disc and to change its resonant frequency upon temperature rise.

Experiment #1 was conducted on a 1" diameter x 1/2" thick disc. Drive voltages up to 50V rms were applied in 10V steps. Final temperatures ranged from 37°C to 105°C. There was little doubt that irreversibility and depoling occurred at the last temperature. Experiment #2 was conducted on a 1" diameter x 1/4" thick disc to realize data for higher surface temperatures. Drive voltages from 30 to 50V rms produced temperatures from 87°C to 127°C. Irreversibility and depoling were quite noticeable at 40V rms.

1.3.3 Interferometer Studies

One of the more obvious methods of measuring vibratory amplitude is the interferometer technique. Gulton's Glennite Interferometer, Model AT-16, was used for these measurements.

Four small mirrors were attached to 1" diameter x 1/2" thick Body 103 ceramic disc 90° apart. Two experiments were conducted on this disc. The first experiment was to correlate displacement or vibratory amplitude with drive voltage. The second experiment was a fixed displacement - drive potential test.

The first experiment gave a radial displacement of 10.4×10^{-6} cm for a drive voltage of 8V rms, and 24.0×10^{-6} cm for 25V rms. This result was precisely reproduced in successive runs. Mechanical Q was calculated for this sample and found to be 240 at 8V and 178 at 25V. The correlation of Q with voltage and displacement is non-linear. This non-linearity was to be further investigated only to an extent necessary for crystal rate gyro application. Two further points are of interest:

(1) An attempt was made to note any variation in displacement at each of the 4 mirror locations due to changes in resonant frequency, drive voltage, sample homogeneity, etc. No changes were evident within the resolution of the measurement.

(2) A strain gage type of measurement, in conjunction with the interferometer technique, which could be used to calibrate the strain gage, would indicate the dependence of vibratory displacement on driving voltage through the range of values in question. Further, some strain method might possibly be sensitive enough to measure any differences in displacement in different directions.

The object of the second test was to observe the effects, using interferometer technique, of extended driving at a fixed displacement (24 x 10^{-6} cm) on a sample of Body 103 ceramic. The experimental set-up was identical to the first test except for the addition of a thermocouple at the surface of the disc to measure temperature and compare it to previous results. The following observations were made:

(1) The final surface temperature compares very closely with that obtained in a previous test (69 - 75°C at 20 - 35V rms against 69°C at 30V rms).

(2) The impedance value was in the range of previous test indicating credence of results, which are reproducible by different test methods.

(3) Impedance and voltage rose with temperature.

(4) Input power remained fairly constant.

(5) Time to reach equilibrium temperature was in the 10 to 20 minute range.

Specific points of interest to crystal rate gyros are:

(1) A warm-up time is associated with the operation of the crystal rate gyro. Therefore, before any measurements can be made, either in the laboratory or in the field, time must be allowed for equilibrium conditions to be reached.

(2) Resonant frequency varies with temperature, although slightly. This condition necessitates use of automatic frequency scanning or feedback in the final system since a change in scale factor will be evident due to off-frequency driving.

(3) Vibration amplitude, which changes with temperature for a fixed drive voltage, also constitutes a change in scale factor. It may be necessary to incorporate automatic volume or displacement control into the final system.

1.3.4 The d_{31} Coefficient

The usual method of determining the d_{31} coefficient of ceramic materials consists of the quite complex procedure of measuring resonant and anti-resonant frequencies, calculating coupling and other quantities, and then, from this data, calculating d_{31}. In direct measurements of the d_{33} coefficient, it had been observed that this coefficient was a function of the force or voltage (heating effects or large signals) used in its determination, and similar dependences might be expected with the d_{31} coefficient. Further, some of the formulae used to calculate d_{31} are derived under certain conditions between the dimensions of the sample. Thus it was deemed simpler and certainly more accurate if some reproducible low force test scheme could be devised to measure d_{31} directly.

The method proposed for measuring d_{31}, the ratio of charge per unit area in the 3 direction to the force per unit area in the 1 direction (in this case, the 3 direction is along the radius of the disc while the 1 direction is normal to the flat faces), consists of a cylinder in which a thick walled piezoelectric ceramic disc is placed and force applied normal to the faces. The sample is polarized and electroded radially and stressed normal to this direction. Thus the charge output in the radial direction is a direct measure of the d_{31} coefficient. Tests of samples 0.5" thick and 0.2" thick under the same load gave consistent ratios of output; under identical loads the output voltages were in the ratio of 5 to 2 as expected. A second test fixture was built, and while the ratios were similar output voltages varied from the original by factors up to 2.

A second and most important reason for setting up this low force testing scheme was to evaluate radially polarized discs. As previously mentioned, it was thought that larger displacements could be obtained by radial polarization and excitation. Subsequent resonant - anti-resonant measurements from which coupling coefficients can be calculated have indicated that a thickness polarization and radial excitation were probably better for crystal rate gyro configurations. The low force testing scheme was then held in abeyance pending further study.

1.4 PIN WHEEL GYRO CONFIGURATIONS

Of all configurations considered, the axle design, and the pin wheel configuration in particular, were deemed the most promising as a practical crystal rate gyro prototype. It consists essentially of a vibrating ceramic disc bonded to a concentric shaft, whose ends are fitted with pinwheels which actuate simple tension-compression sensors connected in series electrically. The analysis of such a configuration is as follows:

Consider a disc of radius r, thickness ℓ, mass M, and density ρ fixed to an axle through its center and rotating about this axis at a constant rate Ω as shown:

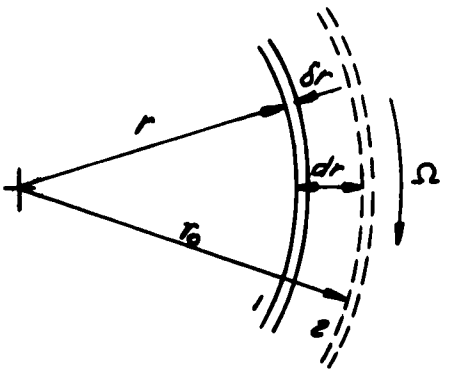

If the disc is now driven radially at its radial resonant frequency ω so that every particle in the disc experiences a radial vibratory motion in addition to the linear tangential motion caused by rotation Ω, an oscillatory torque τ of frequency ω will be developed about the axis. The amplitude of τ can be shown to be proportional to Ω.

In this analysis, the disc is divided into concentric shells of equal mass. Consider one such element of mass dm having radius r and thickness δ r. Here δr is the maximum thickness of the shell in position 1 and the amplitude of motion $dr = r_o - r$. If the moment of inertia of the shell in position 1 is I, and in position 2 is I + dI, then

$$d\tau = I\alpha = \frac{d}{dt} I\Omega$$

or $$d\tau = \Omega \frac{dI}{dt}$$

Now $$I = (dm)\, r^2$$

or $$dI = 2\, r\, dm\, dr$$

thus $$d\tau = 2\, r\, \Omega\, dm\, \left(\frac{dr}{dt}\right)$$

taking $$dm = \rho dV = 2\pi r \delta_r \ell \rho$$

$$d\tau = 4\pi r^2 \ell \rho\ \Omega\ \left(\frac{dr}{dt}\right) \delta_r$$

Since the driving voltage has angular frequency ω, the amplitude of vibration of the outermost shell ($r_o = R$) is $A = r_o - r$, and $r^*(t)$ is defined as $r + dr$, we have

$$r^*(t) \doteq r_o + \frac{r}{R} A \cos \omega t$$

$$\frac{d}{dt}\left(r^*\left[t\right]\right) = \frac{dr}{dt} = -\frac{r}{R} A\omega \sin \omega t$$

Thus the torque contribution of this element becomes

The total torque developed is

$$\tau = \frac{-4\pi A w l \rho \Omega \sin \omega t}{R} \int_0^R r^3 dr$$

or

$$\tau = 2\pi^2 l R^3 \rho A \Omega f \sin 2\pi f t$$

The maximum value of A will be observed when the disc is driven at its natural frequency f_R. Using this value of f and introducing the frequency constant which is defined as the product of the resonant frequency and the resonant dimension C = fR, we obtain

$$\tau = -2\pi^2 l R^2 \rho A \Omega C \sin 2\pi f t$$

Let V represent the maximum value of driving voltage, Q_m the mechanical Q at resonance, and d_{33} the piezoelectric coefficient. Then

$$A = Q_m \cdot V \, d_{33}$$

Note that the disc is assumed to be radially poled, thus validating use of the d_{33} constant for radial vibration. For Body 103 ceramics,

$$d_{33} = 1.1 \times 10^{-10} \frac{\text{coulombs}}{\text{newton}} = 1.1 \times 10^{-10} \frac{\text{meters}}{\text{volt}} = 1.1 \times 10^{-8} \frac{\text{cm}}{\text{volt}}$$

Assuming a drive voltage of 50 volts and a value of 100 for Q_m

$$A = 55 \times 10^{-6} \text{ cm}$$

Other Body 103 constants required are

$$\rho = 5.5 \text{ grams/cm}^3$$

$$C = 140 \times 10^3 \text{ cm/sec.}$$

Then $\tau = -835 \, R^2 \, \Omega \sin 2\pi f t$

and the torque sensitivity in c.g.s. units is

$$\left|\frac{\tau}{\Omega}\right| = 835\ R^2 \text{ dyne cm sec.}$$

If and R are in inches

$$\left|\frac{\tau}{\Omega}\right| = 1385\ R^2$$

Considering a torque pickup system of the tension-compression ceramic rod type as previously mentioned entails corporation of the following details:

(1) The connecting rod between the gyro and sensing elements must be as stiff as possible so as to maximize transmission of torque.

(2) The radius of actuation of the sensors must be as small as practically permissible to create large forces for a given torque.

(3) The sensing elements must have a small capacitance (as Q = CV, and for a fixed charge Q, V will be maximized) and thus must be long and thin (C Area).

(4) The simplest arrangement would be to have the elements mechanically in parallel and two banks of these connected electrically in series thus,

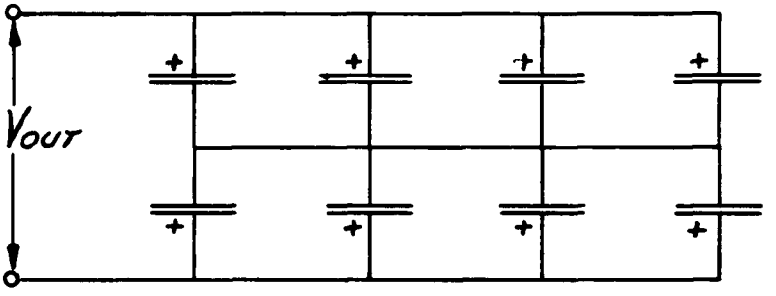

The signs refer to polarization of sensors, not polarity of output. The system may be depicted mechanically thus,

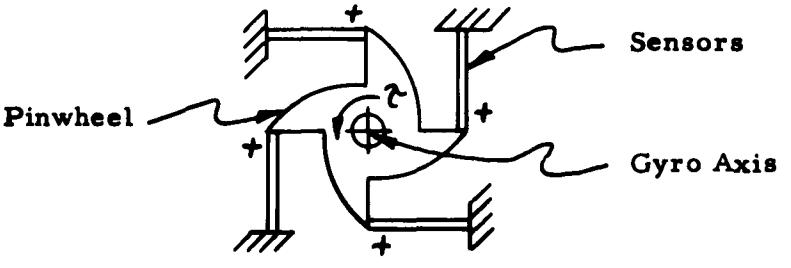

The ceramic sensors should be placed in such a manner that only angular displacements will produce an output, i.e., at right angles to a radius. Only a lateral or a vertical component of motion compresses one pair of elements and extends the other pair, thereby producing opposite and equal electric charges which cancel. The four sensors at the opposite end of the axle are mounted so that a torque which produces compression in the first group causes tension in the second group. Since the two groups of sensors, although connected in parallel (aiding) within the group, are series connected (opposing) with each other, opposite stresses produce additive voltages. This arrangement was selected so that axial displacements which extend all 8 sensors equally would produce a zero output due to cancellation. The analysis of the sensor ceramics is as follows:

If f_i is the force on the i^{th} sensor, and τ_a the applied torque, the voltage output is given as

$$V = \frac{Q}{C} = \frac{(f_1 + f_2 + \ldots . f_8)\, d_{33}}{2\, C_1}$$

where C_1 is the capacitance of a single sensor.

Now $f_1 = \tau / 8\, r$ which gives

$$V = \frac{8\,(\tau/8\,r)\, d_{33}}{2\, C_1} = \frac{\tau\, \ell_s}{2\, \tau\, W^2}\, g_{33}$$

where
- ℓ_s = length of an element
- r = lever arm to the element
- W = width of element
- g_{33} = piezoelectric constant

The dependence of V(t) on the other parameters of this problem are reduced below. Combining the previously derived functions for , A, and V, and using superscripts or subscripts g and s to designate quantities referred to the gyro or sensors respectively, we obtain

$$V = \frac{\pi^2 \ell^g R_g^2 \rho_g Q^g_m V_o d^g_{33} \ell^s g^s_{33} C^g_r \Omega \sin 2\pi f t}{r W^a_s}$$

where
- ℓ^g = thickness of gyro disc
- R_g = radius of gyro disc
- ρ_g = density of gyro disc
- Q_m = mechanical Q of gyro disc

V_o = maximum value of driving voltage
d^g_{33} = piezoelectric modulus of gyro
ℓ^s = length of sensor elements
g^s_{33} = piezoelectric modus of sensors
C^g_f = frequency constant of gyro in radial mode
r = lever arm to sensors
W_s = thickness of sensor (square X-section)
Ω = angular rate to be detected
f = frequency of driving voltage

An estimate of the magnitude of voltage sensitivity was made for a particular unit to investigate possible sizing. The result for a 3" diameter Body 103 disc 2" thick with HT-14 sensors 1/16" x 1/16" x 1" long was:

$$\tau = 62,500 \text{ dyne cm.}$$
$$V(\tau, \ell^s) = 62 \text{ volts}$$

$$\therefore \left|\frac{V_{max}}{\Omega}\right| = 62 \frac{\text{volts}}{\text{rad/sec}} = 1.08 \frac{\text{volts}}{^\circ/\text{sec}}$$

It thus appeared that the pinwheel configuration proposed showed promise and design and construction of such a unit were justified.

A comparison of Body 103 and HT-14 ceramics showed the soundness of the ultimate use of the high temperature material for the entire gyro vibrating system. The properties of these two ceramics are:

Quantity	Body 103	HT-14
ρ^g	5.5 gm/cc	7.2 gm/cc
A_g	24×10^{-6} cm at 30 V rms	48×10^{-6} cm (proposed)
C^g_f	136×10^3 cm/sec	99×10^3 cm/sec
g_{33}	$1.4 \times 10^{-5} \frac{\text{volt cm}}{\text{dyne}}$	$3.4 \times 10^{-5} \frac{\text{volt cm}}{\text{dyne}}$
d_{31}	-0.55×10^{-15} coul/dyne	-0.43×10^{-15} coul/dyne
Curie Point	130°C	375°C

A preliminary estimate of the use of HT-14 for the disc as well as the sensor material indicated the HT-14 ceramic would yield a voltage sensitivity greater than 4 times that of the Body 103 gyro.

One preliminary estimate that seemed a drawback was the capacitance of the ceramic sensors. The circuit output capacitance of proposed sensors totaled 1 $\mu\mu$f. Thus inherent in the system were capacitance attenuation

problems, i.e., an output cable of X μμf would attenuate the output by a factor of X. The proposed use of three conductor coaxial cable would somewhat minimize this condition.

1.4.1 Preliminary Work

Both 4 and 8 element (sensors) designs were considered. However, before actual fabrication could succeed, design parameters for all segments of the system on a more exacting basis were required, considered, and evaluated.

1.4.1.1 Pickup Elements

It was of prime importance to determine the d_{33} piezoelectric modulus for the sensors since these elements respond to compression and tension along their axis. A previous calculation gave a value of $1.4 \times 10^{-15} \frac{\text{coul}}{\text{dyne}}$; however, an empirical determination was necessary due to inconsistencies in production and storage. In addition, poling techniques were probed for maximum sensitivity. A jig was designed and constructed for the d_{33} determinations.

The results of this study showed that the d_{33} of materials supplied was below the $1.4 \times 10^{-15} \frac{\text{coul}}{\text{dyne}}$ value previously utilized, in some cases by a factor of 70. However, by correlation with poling technique, it was determined that repoling at a higher temperature produced materials with a d_{33} coefficient sufficiently close to the assumed value. More important, a device was fabricated that could select and match only those high sensitivity elements needed.

The preliminary study also revealed that preloading of the sensor could increase sensitivity up to 5 times. Obviously, structural strength limits excessive preloading. The initial effort was made with preloading only to the extent it was assured that all elements were always operating in compression.

1.4.1.2 Optimum Thickness to Radius Ratio for Inertial Disc

An experimental investigation of optimum thickness-to-radius ratio was initiated on the following basis. The torque on the inertial disc can be represented by

$$\tau = 2\,MAR_1\,\omega_1\,\omega_2 \cos \omega_2 t$$

This equation is identical to previously derived expressions since

M = mass of disc = $\rho \pi r_o^2$

A = amplitude of radial vibration = $\frac{d_{31}\, r_o\, VQ_m}{\ell}$

R = R_o = equilibrium radius of disc

ω_2 = angular frequency of exciting voltage = $2\pi f_r$

It is evident that torque varies directly with mass. However, certain restrictions were imposed on the dimensions of this member, i.e.,

(1) Target specification of 3" maximum in any direction.

(2) The ratio of thickness to radius must be such that the radial mode possessed the lowest resonant frequency and that the resonant frequencies for the radial and thickness modes were separated by a large enough factor so that cross-coupling during excitation was such that the product of mass times the radial vibratory displacement was optimum (MA).

Frequency constant formulae for both these modes are

$$F^{RD} = \frac{2.03}{2\pi R}\sqrt{\frac{E}{d(1-\sigma^2)}} \quad \text{for the radial mode}$$

$$\text{and } F^{T} = \frac{1}{2t}\sqrt{\frac{E(1-\sigma)}{d(1+\sigma)(1-2\sigma)}} \quad \text{for the thickness mode.}$$

Here F = resonant frequency

R = radius

E = Young's Modulus

d = density

σ = Poisson's Ratio

t = thickness

Using material constants for Body 103 ceramics in the above relation shows

$$F^{RD} \times R = 136 \times 10^3 \ \frac{cm}{sec} = C_l^{RD}$$

$$F^{T} \times t = 250 \times 10^3 \ \frac{cm}{sec} = C_l^{T}$$

C is the frequency constant. It was evident that t must be less than 1.84 R for the radial resonant frequency to be lower than the thickness resonant frequency. An experimental evaluation of the optimum ratio was initiated and included measurement of:

(1) Resonant and anti-resonant frequencies and subsequently the impedance ratio at these frequencies;

(2) Displacement at fixed power input for the various size discs surface temperature.

1.4.2 Four Sensor Crystal Rate Gyro

The four pickup element pinwheel gyro on a turntable is shown in Figure 1. An assembly drawing of the gyro is given as Figure 2a. The design consists of a ceramic disc mounted on a stainless steel shaft which is supported by a pair of miniature ball bearings in a brass fixture. Four piezoelectric elements are mounted between a brass yoke and a shaft support in such a manner as to experience tangential components of torque transmitted by the shaft. The ceramic disc used, 1" in diameter by 0.2" thick, is slipped onto the stainless steel shaft and bonded with epoxy. The pickup elements are similarly bonded between shaft support (form of pinwheel) and yoke. Schematically, the gyro had this form

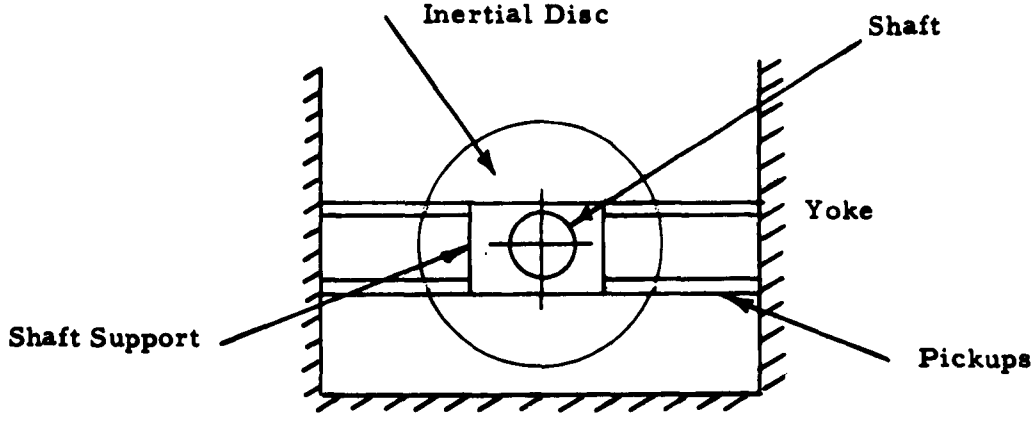

It was previously mentioned that capacitive attenuation was to be expected. One further modification was made: a grounded shield was interposed between the inertial disc and the pinwheel-sensor assembly in an attempt to minimize electrical pickup. The rod pickup elements were thus effectively encased in a grounded box. Before any shielding was introduced, it was noted that pickup from the inertial disc drive oscillator (at the radial resonant frequency of the disc) prevented monitoring of the output voltage from the ceramic sensor elements.

Preliminary test results on this 4 sensor gyro were inconclusive due to electrical pickup, in any case.

1.4.3 Eight Sensor Crystal Rate Gyro

The 8 sensor gyro unit was similar to the 4 sensor unit except that two groups of 4 sensors in shaft supports were employed. In addition, the shaft was of ceramic and the pickup elements were prestressed in compression by means of an adjusting screw and ball applied to the ends of the elements. Shielding was provided as above. Eight pickup elements were selected by use of the low force jig previously mentioned. Their low force d_{33} coefficients were in the range from 0.82×10^{-15} coul/dyne to 0.96×10^{-15} coul/dyne. The

zero rate of turn output for this design was lower than for the 4 sensor unit, although only 4 elements were connected for measurement. This was probably due to a more judicious selection of sensor elements. Representative data for zero rate output versus input voltage to the inertial disc is given in Figures 2 and 3.

The expected output for 4 elements in parallel was V_{max} = 85 mv/°/sec. During preliminary tests on rotating the gyro, the expected output was not realized for either the 4 element or 8 element designs. Thus two problems caused concern:

(1) Zero turn output.

(2) Not obtaining expected output at various turn rates. Even with a 100 or 200 mv bias, 85 mv/°/sec should have been obtained. What was observed was a slight output which may have been capacitive coupling.

1.4.4 Considerations of Signal-to-Noise Ratio for a Complete Crystal Rate Gyro System

The following were considered sources of noise in the crystal rate gyro system:

(1) Measurement limitation - pickup in probes and connecting cables.

(2) Tube noise in electronics system.

(a) Shot Noise - caused by random variations in the emission of electrons from the cathode.

(b) Partition Noise - caused by division of currents between two or more positive electrodes.

(c) Induced Grid Noise - caused by variations in the electron stream passing near grid.

(d) Gas Noise - caused by random variations in the rate of production of ions by collision.

(e) Secondary Emission Noise - caused by variations in the rate of production of secondary electrons.

(3) Thermal agitation - causes shifting of resonant frequency and requires wider bandwidth. Narrowing of bandwidth and lower and more constant temperature is required.

(4) Mechanical asymmetry - causes high zero rate signal by causing the inertial disc to oscillate as a result of unbalance.

(5) Piezoelectric asymmetry - causes variations in deflections and output voltages.

The major contributions to noise were made by (4) and (5). A careful consideration of the mechanical construction of a crystal rate or rotary gyro indicates that precision balance and insensitivity to extraneous loadings, such as bearings or pickup couplings, must be attained for both types of instruments. For the crystal rate gyro configuration used here, eccentricity of a mil in the inertial disc is sufficient to cause noise amounting to large orders of magnitude over the target output level. In addition, the couplings between sensors and the inertial disc and yoke were unsatisfactory in that a rattling and consequent electronic "ringing" would be quite evident. Finally, the bearings on which the inertial member were mounted were poorly secured, leading to excessive bearing torque. The use of bearings rather than a resonant torsional mount also precluded the realization of resonant buildup in displacement, which would improve overall sensitivity.

Piezoelectric asymmetry has the same detriments as unbalance. Variations in deflections in the inertial disc cause acceleration forces which may or may not act through a radius. In the latter case, a noise torque results to decrease sensitivity.

1.4.5 Rate Test Turntable

It was decided that early tests were to be conducted at faster rates of turn than called for in the target spec. Upon achieving satisfactory performance at the higher speeds, more precise and slower rates were to be run on more sophisticated equipment.

The proposed design is shown in Figure 4. It consisted of an aluminum turntable mounted in two ball bearings and was driven by a synchronous gear motor. The aluminum turntable was rim driven from a rubber pulley attached to the motor shaft, and contact was maintained by spring loading the motor mount against the turntable. The speed of this first assembly was 0.6°/sec. Other speeds were obtainable simply by changing the motor pulley.

1.4.6 Further Tests and Considerations

As noted previously, the 8 sensor gyro had a considerable zero turn output. Tests were conducted using various methods of shielding the inertial disc and sensor assemblies, different points of grounding, polarized and non-polarized discs, electronic filtering, and various methods of shielding the input and output of the cathode follower connected to the pickups in an attempt to reduce the electronic contribution to the zero turn output. The conclusions reached from these tests were that in order to achieve minimal electronic signal pickup, three conditions should be met.

(1) Only one side of the gyro should be used (1 set of 4 elements).

(2) The side of the balanced excitation that connects to the side of the disc toward the sensing elements should be grounded.

(3) The side of the disc which assumes a positive electrode under poling should face the sensing element.

For further shielding, the results indicate the following:

(1) Shielding of the disc alone is more effective than shielding of the sensing elements alone.

(2) More effective shielding is effected through use of a shaft of high conducting metal.

(3) It would be advisable to fabricate shields to house the inertial disc and the sensors separately. They should have seamless construction and be of a good conductor material.

(4) These shields should be insulated from each other but grounded together at some judicious external point.

(5) The metal shaft should be insulated from the disc shield but grounded to the sensor assembly shield.

An attempt was made to drive the inertial disc at much lower frequencies than at resonance. Theoretical computations showed this technique produced very small outputs at slow speeds. However, zero rate output was also drastically reduced. Maximum outputs close to 500 μV were observed for rates up to 360°/sec with a zero rate output of 3800 μV. This occurred at a drive frequency of 17.6 KC.

Repeatability runs were made at zero turn rate to establish the stability of the system under a change of discs or sensing elements. These tests showed that repeatability with different components was unattainable, the mismatching of sensors being the main source of trouble. In addition, it may be construed that motions other than torsion existed in these designs.

1.4.7 Concluding Remarks on the Pin Wheel Designs

At this point, it did not appear that pinwheel configurations would approach the requirements specified, and other configurations were investigated.

1.5 OTHER GYRO CONFIGURATIONS AND CONCLUDING WORK ON PHASE I

Two other gyro configurations were considered as possible approaches.

1.5.1 Strain Gauge Sensor Axle Design

This configuration was basically similar to the pinwheel configuration except that strain gauge wires were attached to 2 points on the circumference of the gyro and the variable resistance caused by oscillatory motion of the disc fed through strain gauge amplifiers. Theoretical calculations of this output were of the order of 2×10^{-16} volts and thus unfeasible.

1.5.2 Circumferential Gyro

This gyro configuration was also similar to the pinwheel design. The exception here was that piezoceramic pickup rods were attached to the inertial disc such that the axis of the rod was tangential to the outer diameter. The design seemed to offer two advantages.

(1) It was possible to interpose a connecting piece between the disc and pickup rod thus allowing for better shielding.

(2) It was theoretically possible to cause the output to have double the natural frequency of the inertial disc. Thus zero rate output could be filtered.

As a consequence of the work on the circumferential configurations, a method was devised for synthesizing the torque developed during rotation which could be used in further work. This torque applicator consisted basically of a ceramic element which could be excited at a given frequency and attached to the circumference of any inertial disc of a crystal rate gyro system for evaluation of pickups.

These considerations concluded work on Phase I of the crystal rate gyro program.

2. PHASE II

2.1 SCOPE

A study of the work done in Phase I of the Crystal Rate Gyro program has shown that it was not feasible to build an operating model with any reasonable sensitivity using the piezoelectric disc vibrator in any configuration because of the adverse effects of small motion and high frequency. Work on Phase II was therefore expanded into the expectedly feasible area of high amplitude cylindrically symmetrical vibrators and pickoff devices of high sensitivity. Work in this phase also included methods of minimizing mechanical and electrical noise. Choice of materials and designs was made from the point of view of suitable application to airborne environmental conditions.

It was anticipated that the following objectives could be reached:

(1) A minimum detectable rate of 0.1°/hour.

(2) A maximum sensitivity to acceleration along any axis of 0.05°/hour/g.

The overall objective was to develop an experimental crystal rate gyro that was small, reliable, capable of meeting the above specifications, and had low power consumption.

The expected principal problems included but were not limited to:

(1) Materials and designs for cylindrically symmetrical vibrators.

(2) Torque pickup devices

  (a) Piezoelectric bender elements
  (b) Variable reluctance magnetic devices
  (c) Variable capacitance devices
  (d) Light beam optical output devices

(3) Mechanical noise

(4) Electrical noise

2.2 INITIAL STUDIES

The initial effort was concentrated on three areas:

(1) A critical review of the analytic work carried out in connection with selected existing designs of crystal rate gyros.

(2) The development and fabrication of a complete test facility which included:

(a) The oscillator drive unit
(b) Matching circuitry for coupling the oscillator to the vibrator
(c) The vibrator assembly including as an integral part a cathode follower output
(d) The gyro output amplifier
(e) The output indicator which could be a meter, oscilloscope, or other such device
(f) The rate generating turntable

(3) An investigation of other types of vibratory rate gyros from the point of view of improved sensitivity.

2.2.1 An Evaluation of Maximum Deflection of Pickups for the Inertial Disc Configurations

A critical review of analytic and experimental work previously performed on vibratory disc gyros indicated that such designs are theoretically-empirically not feasible for the vibratory member in a CRG system. A theoretical analysis of the maximum tangential deflection to be expected of the inertial disc under conditions of low turn rates follows.

The device under consideration will be of the simplest type as shown below.

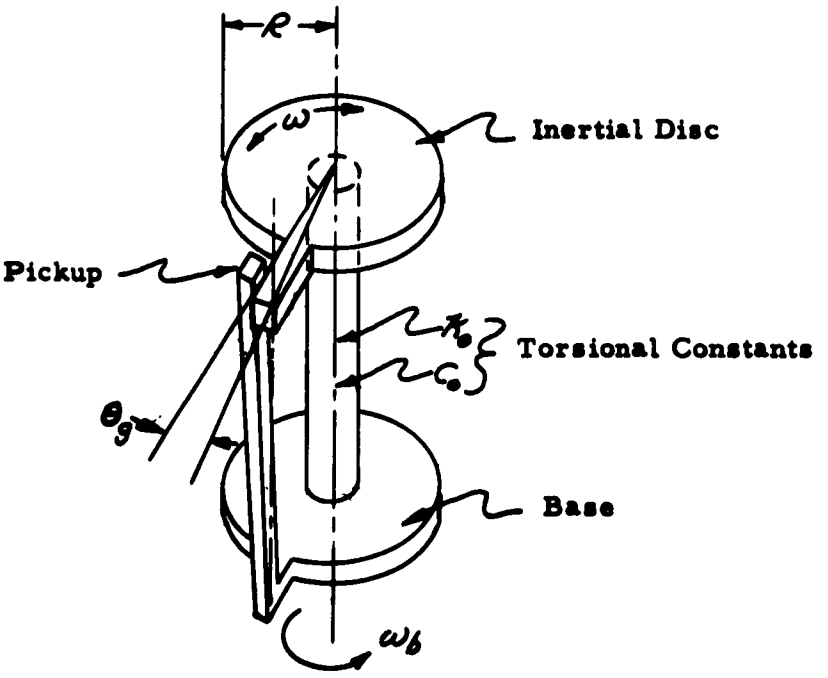

The inertial disc has a moment of inertia whose radius of gyration, is varied sinusoidally at a fixed frequency ω_f. The disc is mounted on a torsion bar of negligible inertia and spring constant K_e. The base is assumed to have an angular rate input of ω_b. It was of interest to investigate the behavior of the pickoff angle (and consequently the tangential deflection) as a fvnction of input angular rate ω_b and other parameters such as I, K_e, C_e. Thus an analysis must include the establishment of the equation of motion and seek its solution.

Define:	I (gm, cm^2)	=	moment of inertia of disc about its axis ($\frac{MR^2}{2}$)
	M (gm)	=	mass of disc
	R_o (cm)	=	radius of unexcited disc
	f_f (cps)	=	excitation frequency
	ω_f	=	2π f_f radians/sec
	t (sec)	=	time
	ω_b(rad/sec)	=	input (base) rate to be measured
	θ_b (rad)	=	$\int \omega_b \, dt$
	ω(rad/sec)	=	angular rate of disc with respect to an inertial reference
	θ (rad)	=	$\int \omega \, dt$
	ω_g(rad/sec)	=	$\omega_b - \omega$
	θ_g (rad)	=	$\int \omega_b \, dt - \int \omega \, dt$
	K_θ($\frac{\text{dyne cm}}{\text{rad.}}$)	=	torsional spring constant
	c_θ ($\frac{\text{dyne cm}}{\text{rad/sec}}$)	=	torsional damping constant
	ω_R (rad/sec)	=	torsional resonant frequency ($\omega_R^2 = \frac{K_\theta}{I}$)
	Q_R	=	torsional Q = $\frac{\omega_R I_o}{c_\theta}$
	R (cm)	=	excited disc radius R = $R_o (1 + \frac{\Delta R}{R} \cos \omega_f t)$

Applying Newton's second law to the disc,

$$K_\theta (\theta_b - \theta) + C_\theta (\omega_b - \omega) - \frac{d}{dt} (I\omega) = 0 \quad (1)$$

Under excitation, the disc inertia may be written as

$$I = \frac{1}{2} MR_0^2 \left(1 + \frac{\Delta R}{R_0} \cos \omega_f t\right)^2 \quad (2)$$

where Δ R is the amplitude of the radial vibration of the disc. Rewriting Equation (1),

$$\frac{d}{dt} (I\omega_b - I\omega) + C_\theta (\omega_b - \omega) + K_\theta (\theta_b - \theta) = \frac{d}{dt} (I\omega_b) \quad (3)$$

or $$\frac{d}{dt} (I\omega_g) + C_\theta \omega_g + K_\theta \theta_g = \frac{d}{dt} (I\omega_b) \quad (4)$$

Equation (4) is a differential equation in ω_g on the left and a forcing function in ω_b on the right. Substituting Equation (2) for I,

$$\frac{MR_0^2}{2} \left[\left(1 + \frac{\Delta R}{R_0} \cos \omega_f t\right)^2 \frac{d\omega_g}{dt} - 2\omega_g \omega_f \frac{\Delta R}{R_0} \left(1 + \frac{\Delta R}{R_0} \cos \omega_f t\right) \sin \omega_f t\right] + \int K_\theta \omega_g \, dt =$$

$$\frac{MR_0^2}{2} \left[\left(1 + \frac{\Delta R}{R_0} \cos \omega_f t\right)^2 \frac{d\omega_b}{dt} - 2\omega_b \omega_f \frac{\Delta R}{R_0} \left(1 + \frac{\Delta R}{R_0} \cos \omega_f t\right) \sin \omega_f t\right] \quad (5)$$

Collecting terms

$$\frac{MR_0^2}{2} \left[1 + \frac{\Delta R}{R_0} \cos \omega_f t\right]^2 \frac{d\omega_g}{dt} + \left[C_\theta - 2 \frac{MR_0^2}{2} \omega_f \left(1 + \frac{\Delta R}{R_0} \cos \omega_f t\right) \sin \omega_f t\right] \omega_g + K_\theta \int \omega_g \, dt =$$

$$\left[MR_0^2 \left(1 + \frac{\Delta R}{R} \cos \omega_f t\right)^2\right] \frac{d\omega_b}{dt} - \left[\frac{MR_0^2}{2} 2\omega_f \frac{\Delta R}{R_0} \left(1 + \frac{\Delta R}{R_0} \cos \omega_f t\right) \sin \omega_f t\right] \omega_b \quad (6)$$

Note that this is an equation of the form

$$f_1(t)\frac{d\omega_g}{dt} + f_2(t)\omega_g + f_3(t)\int\omega_g dt = \omega_b f_4(t) \quad (7)$$

where f_1, f_2 ... are functions of time. In order to simplify the solution, certain reasonable assumptions must be made. These are:

(a) Input angular acceleration is zero $\left(\frac{d\omega_b}{dt} = 0\right)$

(b) $\left(1 + \frac{\Delta R}{R_0}\cos\omega_f t\right) \approx 1$

(c) $C_\theta - 2\frac{MR^2}{2}\omega_f\frac{\Delta R}{R_0} = C_\theta\left(1 - 2Q\frac{\omega_f}{\omega_R}\frac{\Delta R}{R_0}\right) \approx C_\theta$

Equation (6) then reduces to

$$I_0\frac{d\omega_g}{dt} + C_\theta\omega_g + K_\theta\int\omega_g dt = \left[-2I_0\omega_f\frac{\Delta R}{R_0}\sin\omega_f t\right] \quad (8)$$

ω_b

Introduce $\theta_g = \int\omega_g dt$ and obtain

$$I_0\frac{d^2\theta}{dt^2} + C_\theta\frac{d\theta_g}{dt} + K_\theta\theta_g = T\sin\omega_f t \quad (9)$$

where $$T = \left[-2I_0\omega_f\omega_b\frac{\Delta R}{R_0}\right] \quad (10)$$

The steady state solution for θ_g was obtained by standard techniques and found to be

$$\theta_g = \frac{-2\omega_f\omega_b\frac{\Delta R}{R_0}\sin(\omega_f t - \delta)}{\left[(\omega_R^2 - \omega_f^2)^2 + \left(\frac{\omega_R\omega_f}{Q_R}\right)^2\right]^{\frac{1}{2}}} \quad (11)$$

where

$$\delta = +\tan^{-1}\frac{(\omega_R\omega_f/Q_R)}{(\omega_R^2 - \omega_f^2)} \quad (12)$$

For three cases of interest:

$$(A)\ \omega_f \ll \omega_R,\ \theta_g = \frac{-2\omega_f \omega_b \frac{\Delta R}{R_o} \sin(\omega_f t - \delta)}{\omega_R^2} \tag{13}$$

$$(B)\ \omega_f = \omega_R,\ \theta_g = -2\frac{\omega_b}{\omega_R}\frac{\Delta R}{R_o} Q \sin(\omega_f t - \delta) \tag{14}$$

$$(C)\ \omega_f \gg \omega_R,\ \theta_g = -2\frac{\omega_b}{\omega_f}\frac{\Delta R}{R_o} \sin(\omega_f t - \delta) \tag{15}$$

The significant equation is equation (14) where excitation frequency and torsional resonance are "tuned" to equality. Define the peak of θ_g as $\hat{\theta}_g$.

$$\hat{\theta}_g = 2\frac{\omega_b}{\omega_R}\frac{\Delta R}{R_o} Q_R \tag{16}$$

Reasonable parameters based upon fabricated discs were

$\omega_f = \omega_R = (28.1 \times 10^3)\, 2\pi$ rad/sec.

$\Delta R/Ro = 34 \times 10^{-6}$ cm/cm

$Q_R = 10$ (assumed)

Therefore:

$$\hat{\theta}_g = 0.385 \times 10^{-8}\, \omega_b \text{ radians}$$

Assuming it is possible, with reasonable facility, to measure no better than 150 microinches at a 1-1/2 inch radius,

$$\hat{\theta}_{g_{min}} = \frac{R\theta_g}{R_J} = \frac{150 \times 10^{-6}}{1.5} = 10^{-4} \text{ radians}$$

The minimum detectable rate under these conditions then would be

$$\omega_b = \frac{\theta_{g\,min}}{0.385 \times 10^{-8}}$$

$$= 0.25 \times 10^{6} \text{ RAD./SEC.}$$

This figure is extraordinary in light of what was to be expected of the target gyro, and dictated complete abandonment of all ideas and work associated with any vibrating disc designs. Equation (16) points out the requirements of new approaches and configurations. These were:

(a) Low torsional resonant frequency and therefore low excitation frequency ($\omega_f = \omega_R$);
(b) Large change in dimension under excitation, i.e., $\Delta R/R_o$ should be large;
(c) High torsional Q.

The line of thinking led in the direction of mechanical tuning fork configurations using ceramic or electromechanical tines.

2.2.2 Other Vibratory Gyro Types

Three designs, all variations of the tuning fork, were considered and prototypes implemented. These types were:

(a) Split Cylinder: (See Figure 5)

O. D.:	3.94 inches
Wall thickness:	0.255 inches
Width:	1.15 inches
Slot Width:	0.055 inches
$\omega_f = \omega_R$	260 cps

(b) Mechanical Tuning Fork:

This device was to be an electromagnetically excited tuning fork with masses at the ends of the tines. Resonant frequency was to be between 50 to 150 cps.

(c) Ceramic Bimorph:

This approach involved use of one or two ceramic bender elements as tines.

2.2.3 Gyro Rate Generating Turntable

In light of the analytical investigation of 2.2.1, the turntable speed range was extended to a maximum of 350 rpm.

2.2.4 Evaluation of Threshold Sensitivity Goal

The operation of a vibratory gyro may be outlined in the following manner:

An excitation voltage applied to the vibrator causes it to change its radial dimension at a frequency ω_f. This amounts to generating a sinusoidally varying radial momentum. When the vibrator on its mount is rotated at a rate ω_b(ω_b <<< ω_f), the vibrator tends to maintain the same total energy (conservation of angular momentum) regardless of its changing dimensions. The net effect is a torque on the torsional system, which results in a rotational velocity of the vibrating system relative to the base. In this manner, any energy given up radially during a cycle of radial motion is regained by acquiring energy tangentially. The coupling coefficient between the vibrating and torsional system is the base input rate ω_b. Thus, a torque proportional to ω_b, among other parameters, is obtained. This torque acting on the inertial spring-damper torsion system produces a deflection angle θ_g and θ_g is, therefore, proportional to ω_b. The pickoff or readout then converts this angular deflection to electrical signal. A block diagram of the crystal rate gyro is given in Figure 6.

It is of significance to point out qualitatively that while the coupling (as established by ω_b) between the radially vibrating system and the torsional system and hence the readout is relatively weak, the unwanted coupling between the vibration excitation voltage and the readout is, by all experience, relatively strong. In practice, the threshold of sensitivity, resolving power, or resolution is established by the total of all interfering inputs. These include:

(1) Random noise generated anywhere in the system of associated elements, including the readout.

(2) Unwanted (but stable) coupling between any source e.g., the vibration excitation source and the readout.

(3) Wanted or unwanted, but unstable, coupling between a source and the readout, e.g., the effects of temperature dependence and material properties on the output.

In order to reduce the threshold sensitivity to that established by the noise, examination of 2 and 3 above was indicated. The basic approach was:

(1) Make the wanted signal as large as possible by design, i.e., to examine the equation for θ_g and to adjust parameters to yield the largest θ_g for a given ω_b compatible with practical considerations.

(2) Select the proper pickoff which is:

(a) Least sensitive to the known stable or unstable interfering inputs, or
(b) Most sensitive to the desired signal and then attempt electronically to isolate or cancel the known stable interfering inputs.

(3) Reduce the stable or unstable inputs by design, e.g., shielding, temperature control, vibration isolation, etc.

In the equation

$$\frac{\hat{\theta}_g}{\omega_b} = \frac{1}{\omega_R} \frac{\Delta R}{R_o} Q_R$$

it was quite obvious that ω_R must be minimized and $\frac{\Delta R}{R_o}$ maximized for maximum sensitivity. A rough estimate for a proposed tuning fork gyro, operating off resonance, was made in an attempt to establish a practical target and to demonstrate feasibility.

If $\omega_R = 2\pi$ 15 RAD./SEC.

$\omega_f = 2\pi$ 60 RAD./SEC.

$\hat{\theta}_g = 10^{-4}$ RAD.

$\frac{\Delta R}{R} = 0.1$

$\hat{\theta}_g = 2 \frac{\omega_b}{\omega_f} \frac{R}{R_o}$ (for $\omega_f > \omega_b$),

$$\omega_b = \frac{\hat{\theta}_g \, \omega_f}{2 \, \Delta R/R_o}$$

$$= 0.188 \text{ RAD./SEC.}$$

$$= 10.8 \text{ °/SEC.}$$

$$= 1.8 \text{ RPM}$$

This figure was the immediate target. The tuning fork was not to be construed as the final device. It was intended solely as an interim vehicle for the purpose of establishing an operating device which performs as postulated by the theory previously presented. On obtaining the operating device, it would be possible to establish parameters for improved design or more effective measuring techniques. Ultimately, the goal was to measure the target angular rate with a device using piezoelectric elements.

2.3 FIRST TUNING FORK GYRO

Although the Split Cylinder Gyro was fabricated and the Ceramic Bimorph Gyro initiated, all effort was concentrated on the Tuning Fork Gyro. This device was deemed the most promising of all designs considered. A sketch of the first experimental model appears as Figure 7. The basic parameters of the first model were:

ω_f = excitation frequency: 97 cps

ω_R = torsional resonant frequency: 15 cps

This mechanical tuning fork gyro was incorporated into the test set-up illustrated in Figure 8. The tines of the tuning fork were excited by an electromagnetic coil at a frequency of 97 cps from an audio oscillator. The exciter signal, properly amplified in the power amplifier, was biased by means of a 6V battery such that the exciter current varied sinusoidally from zero to peak value but never reversed. The current waveform then was the same as that of DC signal plus an AC whose peak amplitude was just equal to the DC level. In this manner, the magnetic pull on the tines rises to a peak and then drops to zero only once a cycle. Without the bias, the tines would oscillate at twice the exciter frequency.

The first pickup used was a standard Gulton vibration accelerometer of sensitivity 8.8 mV/g. The accelerometer output required the high output impedance of a cathode follower followed by an amplifier. It was

mounted on the tuning fork mount frame such that its sensitive axis was tangent to a circle of rotation of the gyro. A low pass filter was interposed between the cathode follower output and the amplifier input. This filter had a cutoff frequency of 250 cps.

At zero angular rate input to the gyro, the gyro produced an output signal which was quite stable and of the same magnitude as signals produced by an angular rate of from 50 to 100 rpm. This output at zero rate was partially cancelled by an amplitude and phase compensator network as indicated in Figure 6. This compensator is a passive network which attenuates and shifts the phase of the excitation voltage. By addition of the compensator output in series with the filtered and amplified pickup signal, cancellation of the zero rate input signal at the excitation frequency could be effected. However, small and not insignificant second harmonics of the excitation frequency were detected. The filter did eliminate much of the high frequency rattle that was generated and noted in preliminary hookups. With this configuration, clear and direct phase sensitive recognizable output signals roughly proportional to input angular rates of 100 to 400 rpm were attained. Detailed but rough calculations of torsional deflections indicated that the measured signals were approximately 1/10 of that predicted.

This first approach involved an excitation frequency of 97 cps and a torsional resonant frequency of 15 cps. The first attempt to improve performance was then to tune the torsion system to 97 cps by use of a stiffer torsion mount. At a torsional resonance of 85 cps, recognizable outputs were attained for input rates in the range from 30 to 50 rpm.

The displacement of the rotating gyro frame was calculated to be 0.001", sufficient deflection to excite an ordinary ceramic bender phonograph element. The output of such pickups with the above deflection is on the order of several hundred millivolts instead of 5-10 millivolts available from the accelerometer pickup. A standard phonograph bender element then replaced the accelerometer in subsequent tests. A curve of the output voltage with proper compensation versus input angular rate is presented in Figure 9. Data depicting recognizable signals down to the order of less than 10 rpm indicate that, based on noise, it is feasible to repeatedly obtain good results in the range between 5 and 10 rpm. Allowing for a difference between excitation frequency (97 cps) and torsional resonant frequency (the ceramic pickup system had a resonance at 60 cps), this was exactly the order of magnitude of threshold that was set as the target of the first experimental tuning fork gyro.

At this stage, the stability of the unwanted signal became the major factor of contention. This was evident in two ways:

(1) The compensation zero input rate required adjustment at intervals of a few minutes.

(2) The output signal level at zero rate was found to be a function of turntable position.

The first source of instability was presumed to be due to unstable mechanical couplings within the gyro. As this preliminary model was constructed to check feasibility, refined mechanical construction was not stressed. The second source of instability was presumed to be due to mechanical unbalance in the plane of symmetry of the device. This unwanted coupling was also expected to submit to improved mechanical construction, both of the gyro and the turntable.

The first model was then set aside, having served its purpose as a pilot unit. The initial aim was accomplished, and it appeared that the threshold limit for this unit had been reached.

2.4 SECOND TUNING FORK GYRO

A second tuning fork gyro was designed and fabricated. Details of this design are available in Figure 10. This new device represented a significant improvement over the previous unit, specifically along the following lines:

(1) Smaller size

(2) Adjustability of excitation and torsional resonant frequencies - permissible by varying moment of inertia of tuning fork and mount - to design frequency of 71 cps.

(3) Better design and construction to reduce unwanted mechanical couplings at zero input rate.

(4) Flexibility to pickup configurations.

The pickup initially used was a piezoelectric bender element of the phonograph type.

Initial qualitative tests of this unit indicated that the output motion, i.e., motion normal to the base plate, was not purely torsional. There were clearly other modes of vibration including:

(1) Bowing of the leaf spring support

(2) Twisting of the leaf spring support about a horizontal axis.

As a result of these undesirable motions, repeatable data was not obtained. The leaf spring support was modified to relieve this condition. The leaf spring mount then consisted of 4 leaf springs 90° apart connected at the origin and at the extremities. It was anticipated that the "toppling" of the tuning fork, which was mounted at the origin, would be minimized.

Testing of the modified unit indicated that the unit was rate sensitive. However, the position sensitivity of the gyro was still quite evident. This unwanted sinusoidal signal, which exists with the tines excited and the pickup coupled to the torsional system, was cyclic and repeatable. Moreover, this type of signal persisted when the pickup was decoupled from the torsional system and the gyro clamped to prevent torsional motion. Changing the orientation of the decoupled pickup on the base plate resulted in a phase change, but the amplitude remained essentially unchanged. Reducing excitation voltage reduced the level of this noise signal. In the limit, with no excitation of the tines, the signal reduces to a minimum with a wave shape which was random rather than sinusoidal. These results indicated that there was mechanical coupling between the tines and the pickup through the base plate.

To relieve coupling between the pickup and the fork at zero rate, a mechanical low pass filter was constructed. It consisted essentially of a heavy mass mounted on a compliant layer. The stationary end of the pickup was attached to this mass. However, after much modification it was deemed not practical to utilize this unit in the system due to the size of a unit having the required low cutoff frequency.

Further modification of the mechanical stability of the gyro included addition of weights to the tines and an attempt to mount the tuning fork and its nodes. The latter condition will be shown to be impractical in Section 2.6. The added masses lowered the resonant frequency of the fork to 79 cps; the mount was also tuned to this frequency. This frequency was considered sufficiently separated from 60 cps to minimize the line pickup problem.

The modified second turning fork gyro was placed on the test turntable and data taken for various angular rates. This data is given in Figure 11. The table was driven from a synchronous motor through a series of pulleys via a belt drive, and speeds were varied by changing pulley ratios. With this arrangement it was possible to measure the signal output from the turn rate sensor at four distinct speeds, clockwise and counter-clockwise. The following procedure was utilized at each speed:

(1) The drive motor was energized but decoupled from the turntable.

(2) The output signal from the turn rate sensor was recorded (output fluctuated over a moderate range).

(3) The motor was coupled to the turntable via the belt drive and the output signal recorded (output fluctuated over a moderate range).

(4) The motor was de-energized and the output signal recorded. This level corresponds to zero drift rate in the turn rate sensor.

The threshold sensitivity of this instrument, as noted in the figure, is approximately 1/2 rpm, at which point the signal level is slightly above the noise level. The major fault of this and previous units was ineffective mechanical techniques. The testing of this unit concluded activities for Phase II.

2.5 ELECTRONICS

The electronics used in Phase II consisted essentially of commercially available vacuum tube devices. No special electronics of any consequence was employed.

2.6 A NOTE ON NODAL POINTS IN TUNING FORK VIBRATORS

An attempt was made to establish the nodal points or regions in a tuning fork vibrator on a semi-empirical basis in an effort to isolate the vibrating forces of the tuning fork from the base, spring mount, and transducer. A careful theoretical analysis shows this to be impractical when weights are added to the ends of the tines.

Consider a straight beam as shown.

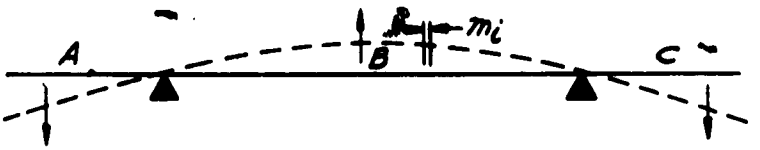

The condition under which a node is located is that the net force exhibited by the algebraic sum of all infinitesimal elements (M_i) of the beam about the node(s) be equal to zero, i.e.,

$$\sum_{i=1}^{n} m_i a_i \text{ (SECTION A)} + \sum_{i=1}^{n} m_i a_i \text{ (SECTION B)} + \sum_{i=1}^{n} m_i a_i \text{ (SECTION C)} = 0$$

This analysis may be effected by calculating the shape of the beam in the deflected position and summing forces along its length. The manner of loading to be assumed should be identical to that in actual use. Nodal points for the straight beam have been determined by many investigators.

Consider a straight beam with masses at the ends as shown.

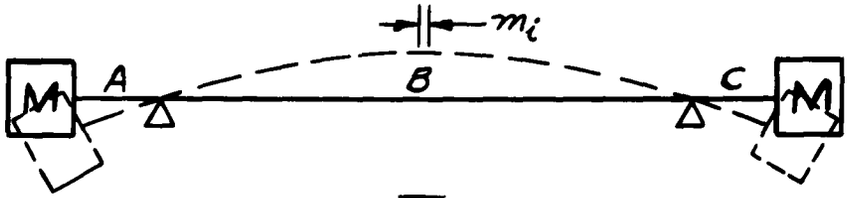

$$M \gg \sum_i m_i$$

If the condition $M \gg \sum_i m_i$ is imposed, and the conditions

$$\sum_{i=1}^{n} m_i \cdot a_i \text{ (section A)} + \sum_{i=1}^{n} m_i \cdot a_i \text{ (section B)} + \sum_{i=1}^{n} m_i \cdot a_i \text{ (section C)} = 0$$

are to be met, it can readily be seen that lengths A and C approach zero as $\sum m_i / M$ approaches zero. Thus, the mount must be placed at or near the added masses. This is contradictory in that the masses would be restrained, and the magnitude of the change in inertia for such a unit rotated about an axis parallel to its length would approach zero. The result would be a complete loss of sensitivity to turn rate.

The foregoing analysis is similar for the tuning fork with the exception that the straight beam assumes the shape of the letter U. The force balance remains the same and in the case of added masses at the tips of the tines, the nodes are located in the masses as for the straight beam. The result as postulated is that the notion is impractical.

A second point to be considered, should the location of a node be practical, would be the stability of a node. It is a well established fact that the nodes of a straight beam are not stationary when measured along a coordinate. Only if the distance between nodes is measured along the curved length of the beam when deflected would this distance be constant. Thus, flexible mounting would have to be incorporated. This would only add to the mechanical instabilities already apparent in a vibratory gyro.

2.7 A NOTE ON THE SINGLE TINE SYSTEM

A preliminary analysis of a single tine vibrator was made to investigate the possibility of such a design as a rate sensor. The analysis was given impetus since it was previously indicated that $\theta_g \sim \frac{R}{R_o}$, and the single tine system theoretically gives a minimum R_o. In addition, it was known that the single tine system gave a second harmonic output when subjected to turn rate and a fundamental when still; thus, filtering could reduce zero rate output to a minimum. However, only a preliminary investigation was made.

PHASE III

3.1 SCOPE

The results of Phase II indicated clearly the feasibility of high amplitude cylindrically symmetrical vibrators for the inertial member of a vibratory rate gyroscope system; in particular, the tuning fork configuration of high inertia and low resonant frequency. The work of Phase III was then devoted to refining the tuning fork system both mechanically and electronically.

Mechanically, the configuration was to be made insensitive to motions about other axes and be of precision fabrication to insure maximum stability and low mechanical noise. In addition, a resonating mount of high mechanical Q was to be developed to increase sensitivity.

Electronically, a precision null system was to be developed together with an optimum pickup for low zero input rate signal or noise. The electronics to be developed were to require a minimum of size and power consumption.

The overall objectives to be achieved for Phase III were basically the same as for Phase II, viz;

(1) A minimum detectable rate of 0.1°/hr.

(2) A maximum sensitivity to acceleration along any axis of 0.05°/hr/g.

(3) Smallness, reliability, and low power consumption.

3.2 THEORETICAL RE-EVALUATION

In order to obtain a more exact determination of principal parameters for the precision design of a tuning fork gyroscope system, a thorough theoretical analysis of this configuration was made based on the exact geometry involved. This analysis follows:

Consider the tuning fork configuration shown below in its simplest form:

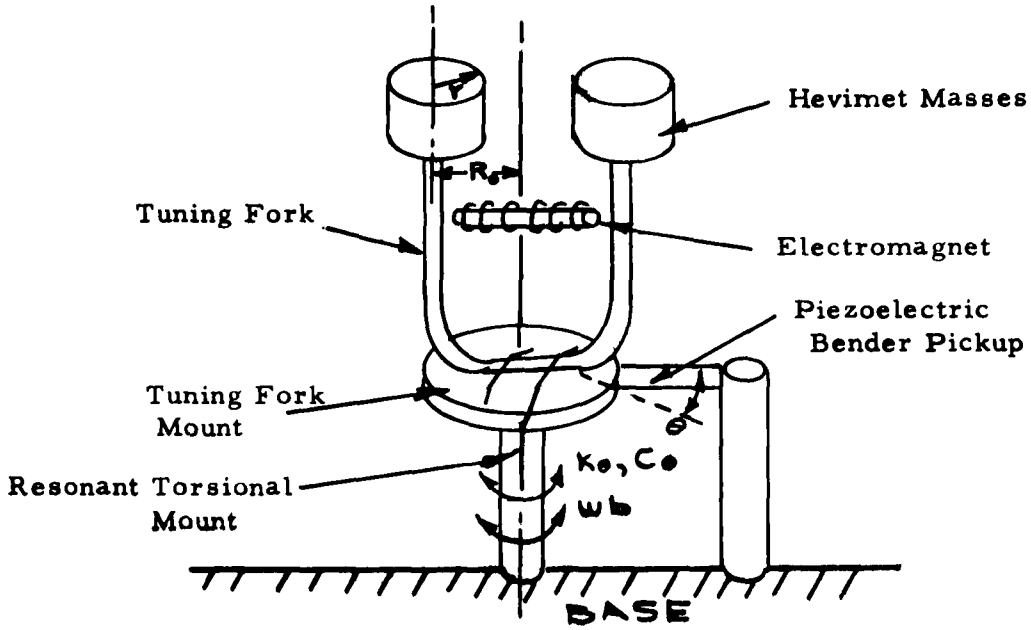

The tuning fork is secured to its mount and loaded with the Hevimet weights at the ends of the tines. The tuning fork and its mount are mounted to a resonant torsional mount of elastic constant K_θ and damping C_θ. The tuning fork is vibrated electromagnetically through a displacement ΔR at its resonant frequency ω_f. It is desired to determine the displacement of the tuning fork and its mount (inertial member) relative to the base as a function of a constant input angular rate ω_b, and other constants R, ΔR, M, ω_f, C, and ω_n, the undamped natural frequency of the torsional mount.

The inertia of the tuning fork and its base is assumed to be that of the masses alone since the masses are large and have a specific gravity of 19. This inertia is, for the two mass tuning fork,

$$I = 2\left[\frac{1}{2}Mr^2 + M(R_o + R\sin\omega_f t)^2\right]$$

$$= 2\left[\frac{1}{2}Mr^2 + MR_o^2\left(1 + \frac{\Delta R}{R_o}\sin\omega_f t\right)^2\right] \qquad (17)$$

A reasonable assumption is made for I_o, which determines the undamped resonant frequency of the torsional mount. This is

$$\left(1 + \frac{\Delta R}{R_o}\sin\omega_f t\right)^2 \approx 1$$

Thus: $I_o = 2\left(\frac{1}{2} M r^2 + M R_o^2\right)$ (18)

The equation of motion for thesystem is

$$I_o \frac{d^2\theta}{dt^2} + C_\theta \frac{d\theta}{dt} + K_\theta \theta = \tau \quad (19)$$

where $\tau = \frac{d}{dt}(I \omega_b)$ (20)

Since ω_b is constant

$$\tau = \omega_b \frac{dI}{dt} = 2M\omega_b \left[2\omega_f R_o \Delta R \cos \omega_f t + 2\omega_f \Delta R^2 \sin 2\omega_f t\right] = 4M\omega_b \omega_f \Delta R (R_o \cos \omega_f t + \Delta R \sin 2\omega_f t)$$

Assuming reasonably that $R_o \cos \omega_f t \gg \Delta R \sin 2\omega_f t$

$$\tau = 4M\omega_b \omega_f R_o \Delta R \cos \omega_f t \quad (21)$$

Now $I_o \frac{d^2\theta}{dt^2} + C_\theta \frac{d\theta}{dt} + K_\theta \theta = 4M\omega_b \omega_f R_o \Delta R \cos \omega_f t$ (22)

let $A = 1 + \frac{1}{2}\left(\frac{f}{R_o}\right)^2$ (23)

then $I_o = 2AMR_o^2$ (24)

Rewriting equation (22).

$$\frac{d^2\theta}{dt^2} + \frac{C_\theta}{I_o}\frac{d\theta}{dt} + \omega_n^2\theta = \frac{2\omega_b\omega_f}{A}\frac{\Delta R}{R_o}\cos\omega_f t \qquad (25)$$

where $\omega_n = \sqrt{\frac{K_\theta}{I_o}}$, the undamped natural frequency of the torsional mount.

Assume a solution of the form $\theta = X \sin \omega_f t$

then $\frac{d\theta}{dt} = \omega_f X \cos\omega_f t$

$$\frac{d^2\theta}{dt^2} = -\omega_f^2 X \sin\omega_f t$$

So $$-\omega_f^2 X \sin\omega_f t + \frac{C_\theta}{I_o}\omega_f X \cos\omega_f t + \omega_n^2 X \sin\omega_f t = \frac{2\omega_b\omega_f}{A}\frac{\Delta R}{R}\cos\omega_f t$$

Since ω_n and ω_f are to be equal for maximum Q.

Thus $$X = \frac{2I_o\omega_b}{C_\theta A}\frac{\Delta R}{R_o}$$

and $$\theta = \frac{2I_o\omega_b}{C_\theta A}\frac{\Delta R}{R_o}\sin\omega_f t$$

$$= \frac{4M\omega_b R_o \Delta R}{C_\theta}\sin\omega_f t \qquad (26)$$

Defining the peak of θ as $\hat{\theta}$ we obtain

$$\hat{\theta} = \frac{4 M \omega_b R_o \Delta R}{C} \tag{27}$$

The significant result obtained shows that the system is independent of ω_n and ω_f except that they must be equal. Other parameters dictated were:

(1) M was to be maximized (a material of specific gravity was to be used for the masses).

(2) R_o was to be limited only by size considerations.

(3) ΔR was to be limited only by fatigue limit of tuning fork material for 10^{10} cycles.

(4) The resonant mount must be of high mechanical Q to minimize C.

(5) A low ω_f was desirable for two reasons: longer life of the tuning fork and low power consumption.

The considerations derived above dictated the design of the first precision tuning fork gyroscope system of Phase III. It was anticipated that practical knowledge gained in the first model would expedite building and testing the subsequent precision model.

3.3 FIRST PRECISION TUNING FORK GYRO SYSTEM

3.3.1 The Tuning Fork

Based on the foregoing theoretical analysis, a first design was made using the following parameters:

ω_f = 50 cps

M = 1.6 lbs.

R_o = 1.00 in.

ΔR = 0.04 in.

The tuning fork was fabricated by a precision machine shop. The important tolerances for a precision tuning fork are the alignment of the center of the fork and the centers of the masses. All three center lines must lie in the same plance for optimal results. In addition, the plane of these centers must be parallel to the central axis of rotation and centered on the torsional mount. Unfortunately, the first fork was found to be 0.012" out and contributed much to noise or zero rate output.

The significance of this unbalance may be shown simply. Consider the line of centers of the masses of fork as shown.

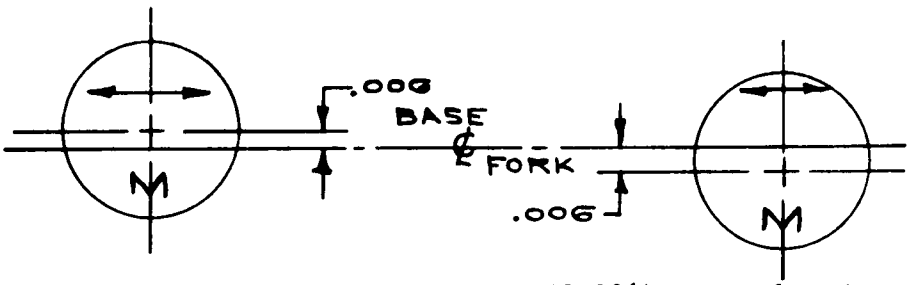

It is clear that a couple amounting to 2 M (0.006) in pounds exists even at zero input angular rate and thus masks the threshold sensitivity of the system.

Modification was made to the masses which allowed minor alignment of these centers. This modification consisted essentially of taps in the weights which allowed the addition of small weights on one or both sides of the mass. Using this technique, a null output of 100 millivolts was achieved at the pickup.

3.3.2 The Torsional Mount

It was desired to develop a torsional mount which, in the ideal, was compliant in the torsional sense and extremely rigid or insensitive to other motions. The two crossed springs used in Phase II had one virtue, ease of adjustment for resonant frequency. However, this mount was not resistant to sway, a major source of mechanical noise, and therefore of little use for the massive fork contemplated. Adjustment of resonant frequency is a minor problem in development, in any case.

After much thought and experimentation, a mount close to the ideal was developed. This mount, shown below simply, consists of

two circular plates, one to which the fork is mounted, separated by three or more flat springs which are oriented on radii.

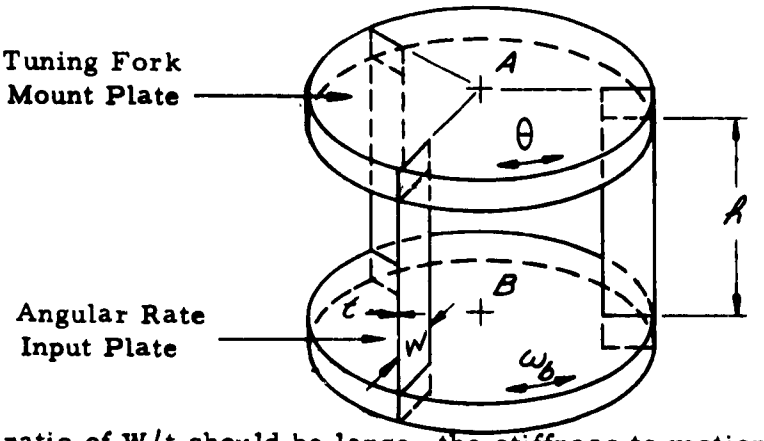

The ratio of W/t should be large, the stiffness to motions other than torsional increasing with W/t. The resonant frequency was varied by adjustment of h after the fork was mounted in place at the center of plate A. Once equal resonance was obtained between fork and mount, the springs were secured with epoxy cement. After initial fastening the fork mount was also secured with epoxy. Resonant frequencies were measured using ceramic piezoelectric bender elements attached to one tine of the tuning fork and plate A of the torsional mount.

It was desirable to utilize spring materials with minimum loss. Spring manufacturers were consulted in an attempt to uncover a spring material of the highest Q known. However, these proved fruitless as this property is not a widely known quantity. In lieu of this knowledge, materials with very high elastic limits were used as Q varies directly with this property.

3.3.3 Mounting the Tuning Fork

Expedience was a governing factor in mounting the tuning fork on this first precision gyro. The fork was simply clamped at its center and statically balanced on precision ball bearings with an auxiliary fixture. Dynamic balance was achieved electrically using addition of small weights and piezoelectric bender elements as previously mentioned.

It was originally intended to mount the fork at its nodes. However, calculation of nodes and the designing of a mount were considered too time consuming. In subsequent studies, this notion proved to be impractical (see 2.6). It is only possible to decrease the transfer

of vibration from the tuning fork vibrator; it cannot be eliminated without additions to the system. Should elimination be required, a dynamic absorber almost equal in size to the tuning fork would be an obvious solution. Size permitting, two in-phase tuning fork vibrators, oriented back to back, would be ideal; efficiency per unit size would not decrease since sensitivity would double.

3.3.4 The Pickup System

Expedience also governed the choice of a pickup system. It was desired to obtain data on the threshold sensitivity of the gyro system by brute force techniques, if necessary. The ceramic piezoelectric bender was an extremely simple device. No electronic circuitry was required for actuation, allowing for quick results. This pickup is not without disadvantages. It was temperature sensitive and lowered the Q of the mount by loading. One side of the bender pickup element was connected rigidly to the tuning fork mounting plate (plate A of the torsional mount) by means of an arm fastened to the plate. The other end of the pickup was rigidly mounted to a post on the base or turntable. The ceramic piezoelectric element used was a bimorph type as used in phonograph pickups and had dimensions 0.021" x 1/2" x 1-1/4", thickness poled. The output of this sensor was monitored by a Ballantine voltmeter and a Hewlett-Packard oscilloscope as required.

3.3.5 Tuning Fork Electromagnetic Drive

The tuning fork was set into vibration by means of an electromagnet placed between the tines, attracting the tines at a fixed frequency. Originally, the fork was driven by an external audio oscillator through a power amplifier. It was soon apparent that continual adjustment of the oscillator was required in order to keep the fork at resonance. Since the Q of the fork was 500, slight drift of the oscillator caused a large change in R. The logical step was then to incorporate the fork into a feedback loop, thus allowing the fork to choose its own resonant frequency as the drive frequency.

Transistor circuitry was chosen for its small size and reliability. Details of this circuit are presented in Figure . As shown in this schematic, there is a pulse of current once each cycle, and thus no provision to shift AC to avoid driving the fork twice each cycle is required. The input to the amplifier is derived from a small ceramic piezoelectric bender element which was cemented to one tine of the tuning fork. Proper phasing is required to sustain oscillation. The amplitude of vibration, ΔR, was controlled by varying input resistance. A choice

of 0.04" for ΔR was made. The output of the amplifier was connected to the coil of the electromagnet.

3.3.6 Initial Testing

The mechanical configuration of the gyroscope system may be seen in the accompanying photograph, Figure . The entire system is mounted to an aluminum plate for ease of transport. The attempt to achieve a null by dynamic balancing with weights resulted in a reading of 100 millivolts at the piezoelectric bender. Rough testing of the unit on a crude turntable of minimum speed 0.04°/sec showed the unit to be rate sensitive even at the lowest speed. However, readings were questionable in light of the test apparatus used.

Further tests were run on a Genisco turntable made available at Bendix Aviation, Teterboro, New Jersey. Test results here were enlightening. While testing for rate of turn response, a sensitivity to tilt was observed. After the rate of turn response was recorded, a check on the effect of tilt was made. In addition, the gyro was found to be position sensitive.

The Genisco table was found to be slightly tilted and its motion non-planar. Also, no provision was made to isolate it from the environment. Such normal environmental conditions as closing of doors caused jarring of the table. These conditions showed the unit to be too sensitive to shock. Readings were made under optimum conditions, i.e., no shocks and minimum tilt.

The rate of turn response was linear as predicted. A plot of these data are given in Figure . The lowest rate of turn output measured or threshold sensitivity appeared to be 0.05°/sec. at which point the output was somewhat obscured by pickup of ambient shock and vibration. Note that the dynamic range of the gyro system is on the order of 60:1. This was due to saturation of the flat springs of the torsional mount, i.e., the spring was driven into the region of non-linearity. The dynamic range of this torsional mount may be extended by increasing the thickness of the springs, and consequently increasing their length to maintain the same resonant frequency.

Sensitivity to tilt was checked by mounting the gyro system to a gyro tilt table. The deflection of the fork, as tilt increased to 90°, was monitored by a dial indicator gauge of sensitivity 0.0001" per division. A comparison of calculated deflection to observed deflection showed the observed deflection to be slightly higher. The difference was attributed

to shifting of the fork in its clamp and later verified. The observed deflection of 0.003" at 90° was sufficient to cause a very high null reading in any case. In addition, the null reading increased sharply at small angles of tilt and flattened off at maximum tilt. This deflection under tilt must be minimized.

The position sensitivity of the unit is shown in Table II. As previously mentioned, the motion of the Genisco table was not quite planar (attributed to poor bearings) and somewhat tilted. The effects of tilt and shock (due to bad bearings) are discussed above and partially, at least, explain this phenomenon.

3.3.7 Electronic Circuitry

The rate sensitivity of this first precision tuning fork gyroscope system was verified. The major obstacle to increased sensitivity, other pickups notwithstanding, was the excessive null output at zero rate. The logical step was then to incorporate circuitry which ideally amplified the change in output voltage. To achieve this end meant subtracting a voltage approximately adjusted in phase and amplitude from the present null output signal. Theoretically, at least, it was possible to obtain zero output for zero angular input rate, despite mechanical unbalance.

The solutions to the problems raised in seeking to null the zero rate output voltage served as solutions to all the electronic requirements.

It is a simple matter to subtract any two voltages provided both are identical in waveform. Practically speaking, however, a complex waveform is difficult to duplicate; this was the condition that existed here. To counteract this condition, a filter was devised to extract the fundamental only, this being sinusoidal. Coils at 50 cps become excessively large, and attention was directed toward active filters incorporating only resistors and capacitors. To achieve the initial null, a Twin Tee selective feedback amplifier was developed.

With vacuum tube Twin Tee amplifiers, the filter network is driven from low impedance and terminated in extremely high impedances (usually open grids). The significant parameter is E_o/E_i. A plot of this against frequency has a sharp null at one frequency. Phase shift is from +90° to -90° around the null. If the output of a vacuum tube amplifier is fed back negatively through such a network, there will be one frequency with no negative feedback, and thus a maximum output will exist at this frequency. With transistors, the impedance relations are opposite from those of the vacuum tube, i.e., transistors have high output impedances and low input impedances. Since transistors are current devices, and a

plot of I_o/I_i for the transistor device will have the same frequency plot as E_o/E_i for the vacuum tube device, it is possible to obtain the same results with transistors. Instead of constant voltage drive, constant current drive is used, and instead of open circuit termination, short circuit is used.

The transistor was found to be well suited for Twin Tee current feedback. A schematic for the electronics system is given in Figure . The configuration chosen provides the proper conditions. The series 100K resistor, despite a consequent loss in gain, sharpens the Q of the circuit. This Q is 20, and the voltage gain from input to the 100K to the output is 10. This couplet was used as a basic amplifier to meet all the remaining electronic requirements.

A block diagram of the electronics system is presented in Figure . The output of the ceramic piezoelectric pickup element was fed to a frequency selective amplifier (described above). The resultant sinusoidal output became one input to a differential amplifier. The output from this variable gain, variable phase amplifier was adjusted in amplitude and phase to produce a minimum or null output from the differential amplifier under zero angular rate input conditions at the gyro. This output was then fed through two cascaded frequency selective amplifiers, and the resultant output was monitored on a Ballantine VTVM.

The variable phase, variable gain amplifier consisted essentially of an emitter follower to provide a low output impedance for the phase shift network. Assuming that the network is driven from a constant voltage source, a simple analysis will show the phase shifting property. The signal into this amplifier was derived from a piezoelectric element cemented to one tine of the tuning fork. This voltage is sinusoidal.

The differential amplifier consists of three transistors, one of which serves as a high incremental impedance in the emitters of the other two. The advantage gained is that the currents permitted to flow ensure that all transistors operate with high β rather than starved values of β.

3.3.8 Further Testing

It was decided to use sidereal rate as a standard rate of turn. Toward this end, the test turntable was modified to provide a rate of 0.0039°/sec and the electronics completed and debugged.

Upon optimal adjustment of phase and amplitude at the variable gain, variable phase amplifier, a system null of 70 mV was

achieved, including residual harmonics. The response to a rate of turn of 0.0039° sec was a change of 2 volts. By increasing gain, a change of 12 volts was achieved. At this point, saturation of the circuitry occurred.

The sensitivity of the system was encouraging. However, serious drawbacks were observed. These were:

(1) The null voltage, after rate of turn was removed, did not return to the original value.

(2) The null voltage did not remain constant with time under zero rate conditions.

(3) The large, cantilever supported masses were very sensitive to shock and vibration.

To alleviate condition 3, the test turntable was placed on four shock mounts with a system natural frequency of 8 cps. This decreased the mechanical pickup and consequent electronic pickup by 20 db, allowing the readings given above to be repeatable under optimum conditions of nulling. It should be borne in mind that this sensitivity to shock and vibration is exaggerated by the initial mechanical unbalance of the gyro and is not to be expected of a true precision fork. This sensitivity is also exaggerated by the extreme length of the tines.

The cause for a change of null voltage after removal of input angular rate appeared to be directly related to tilt. It was noted that large output changes at zero rate occurred when tilt was impressed, e.g., when a person leaned on the bench supporting the test turntable. This agreed with previous notations and measurements made at the Bendix facilities. It should be noted that the output changes as a function of tilt were made at the pickup, with no electronic gain. The addition of gain would show this change to be tremendous. It was also felt that tilt was exaggerated by non-planar motion of the turntable as a result of faulty bearings. The incidence of flats and other non-spherical distortions are high for a radial ball bearing which is loaded axially. Very slight out-of-roundness of the balls is sufficient to cause non-planar motion. In addition, flats will cause minor shocks in the rotary sense. All the foregoing contribute, in some magnitude, to the observed change in null upon removal of angular rate. The output signal tended to return to its original value as the gyro was rotated back to its original position, but a slight hysteresis was noted in many instances. It is felt that superior test equipment would obviate much of the difficulty noted above.

The problem of null drift with time with zero input rate was related to temperature change. After repeated measurements of the two input signals to the differential amplifier, it was concluded that null voltage was temperature dependent. To verify this conclusion, a continuous record was made of temperature and the output of the differential amplifier, using a two-channel Sanborn recorder and a thermistor driven by an audio oscillator. The results of these tests over several days of continuous tests verified this conclusion. The output varied directly with temperature and increased with increasing temperature until saturation of the circuitry occurred in every case. An investigation of ceramic materials indicated that these materials were unsatisfactory for this application.

Due to this temperature dependence, repeated nulling of the circuitry was required. As a consequence, the variable phase, variable amplitude amplifier was modified to simplify this adjustment. The signal input to this amplifier was derived from the null output signal in this modification; the original input from the tine was disconnected. This arrangement allowed for fixed phase input relative to null output, and allows for a simpler null adjustment (amplitude only). This has been successfully accomplished.

3.4 RESULTANT SECOND PRECISION GYROSCOPE SYSTEM

It was felt that the first precision gyro had served its purpose. It was possible, under optimum conditions, to measure the target rate. The sensitivity of the instrument is unquestionable. It remained to develop a new vibratory gyroscope system which would obviate the problems encountered above. Toward this end, the experience gained in the construction and testing of the first unit was invaluable.

The basic parameters arrived at or to be modified included the following:

(1) Shorter times to alleviate exaggeration of the tilt effect.

(2) One piece construction of the tuning fork and its mount.

(3) Mounting of the tines at a "quasi-node" to decrease coupling of this vibration.

(4) Longer flat springs of the same resonant frequency in the torsional mount to increase isolation to shock and vibration in all axes by virtue of improved columnar dimensions.

Theoretically, sensitivity to shock and vibration varies as $1/\ell$, where ℓ is the length of the flat spring for the same resonant frequency. It was observed and theoretically confirmed in a previous experiment that buckling and permanent set would occur for very thin springs, lending credulence to shock susceptibility.

(5) High accuracy in alignment of the critical center lines of the masses and the fork into a single plane.

(6) Development of a non-loading pickup.

(7) Eliminate ceramic piezoelectric pickups of any kind.

(8) Slight lowering of the resonant frequency of the system, within reason.

The second precision tuning fork gyro, designed to incorporate all the improvements indicated by the conclusions arrived at in the first unit, is shown in Figure . The tuning fork and its mount is precision machined as a single unit and acts as one plate of the torsional mount. The line of centers of the masses and the center of the fork are within ±0.0001" measured at the centroid of the masses. The central section of the fork has been relieved to form a "quasi-node". The material of the fork and mount is 7075-T6 aluminum alloy, heat treated to a strength of 85,000 psi. The tines have been shortened to decrease deflection under tilt 65%. The resonant frequency of the system with these modifications has been lowered to a calculated 41 cps. The ceramic piezoelectric element originally cemented to a single tine to keep the electromagnetic drive has been replaced by a quartz element to avoid temperature complications. The flat springs of the torsional mount have been increased in thickness by a factor of 8, thus decreasing sensitivity to shock and vibration. Overall package size of the unit including most of the electronics is 3.950" diameter x 4-3/8" long.

The major developmental area was the pickup. On the basis of data obtained from the National Bureau of Standards, a capacitor pickup which can sense deflections on the order of 10^{-9} cm under optimum conditions has been designed. The pickup consists essentially of two plates (gold plated for maximum Q), one fixed to the base and the other moveable with the tuning fork and mount. This constitutes a variable capacitor where the change in capacitance is a function of separation of the plates. This capacitance is fed to a bridge excited by a 400 KC carrier. The bridge is balanced at zero input rate. Any motion then

will modulate the 400 KC. This pickup will be temperature independent to a much greater degree than the ceramic piezoelectric element originally used. In addition, little or no loading to the system will prevail, thus sharpening the mechanical Q of the system and increasing the sensitivity to angular rate.

In summarizing, it should be reiterated that sensitivity, even to the target rate, has been achieved in the first precision tuning fork gyroscope system. What remains is to eliminate the instabilities outlined above. To a great extent, the solutions to these problems have been designed into the resultant second unit. It is expected that the second unit will surpass the original in sensitivity. There is no doubt that the problems encountered in the first unit will be decreased significantly in the second.

REFERENCES

1. Wiley, C., "Design of a Vibrating System for the Detection of Angular Rate", W33(038) ac-14153, Goodyear Internal Report dated April 10, 1952 (GER, 12-4).

2. Deuser, D.A. and Hawranick, M., "Summary of Work Done on Crystal Rate Gyro", Report No. 49808, Goodyear Internal Report dated May 13, 1955.

3. Clevite Corporation - Melvin Kullin, "Interim Summary Report on Piezoelectric Rate-of-Turn Indicator", Contract Nonr-2210(00), ONR, May 1, 1957.

4. First Engineering Proposal submitted by Gulton to WADC on May 16, 1957.

TABLE I

REPORTED CHARACTERISTICS FOR VIBRATORY RATE GYROS

Reference	Configuration	Frequency	Driving Voltage	Residual Output at Zero Turn Rate	Sensitivity (mv/°/sec.)	Zero Turn Output / Sensitivity/°/sec.	Stability
2	Disc & Torque Tubes	100 KC	25 V	20 mv & 2 V *	-	-	-
3	Tuning Fork	200 cps	2 V	0.1 V	0.1	10^3	Fair
3	Twin Bender	110 cps	10 V	18 mv	0.03	0.54×10^3	Poor
3	Vibrating Reed	400 cps	2 V	0.2 V	0.06	3.3×10^3	Poor
3	Ring & Cylinder	43 KC	100 V	4.0 V	0.1	40×10^3	Very Poor

* Different bonding agents used.

TABLE II

ZERO RATE OUTPUT VOLTAGE VERSUS POSITION FOR THE PHASE III TUNING FORK GYRO

Angular Position	Zero Rate Output Voltage (mv)
0	355
15	284
30	225
45	212
60	188
75	200
90	240
105	240
120	225
135	284
150	355
165	396
180	420
195	420
210	374
225	374
240	355
255	355
270	374
285	374
300	374
315	374
330	374
345	374
360	374

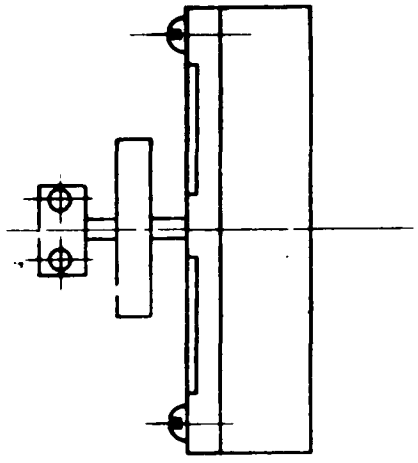

TOP

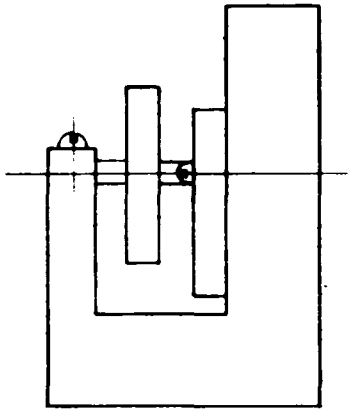

SIDE

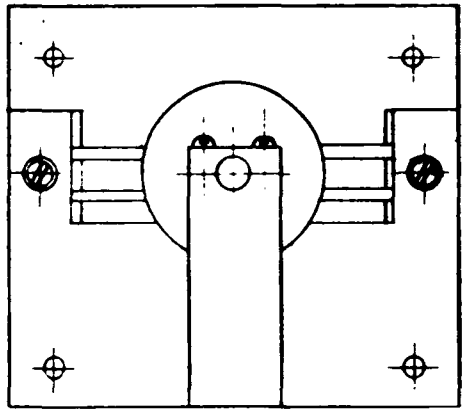

FRONT

FOUR ELEMENT X-TAL RATE ASS'Y

FIGURE 1

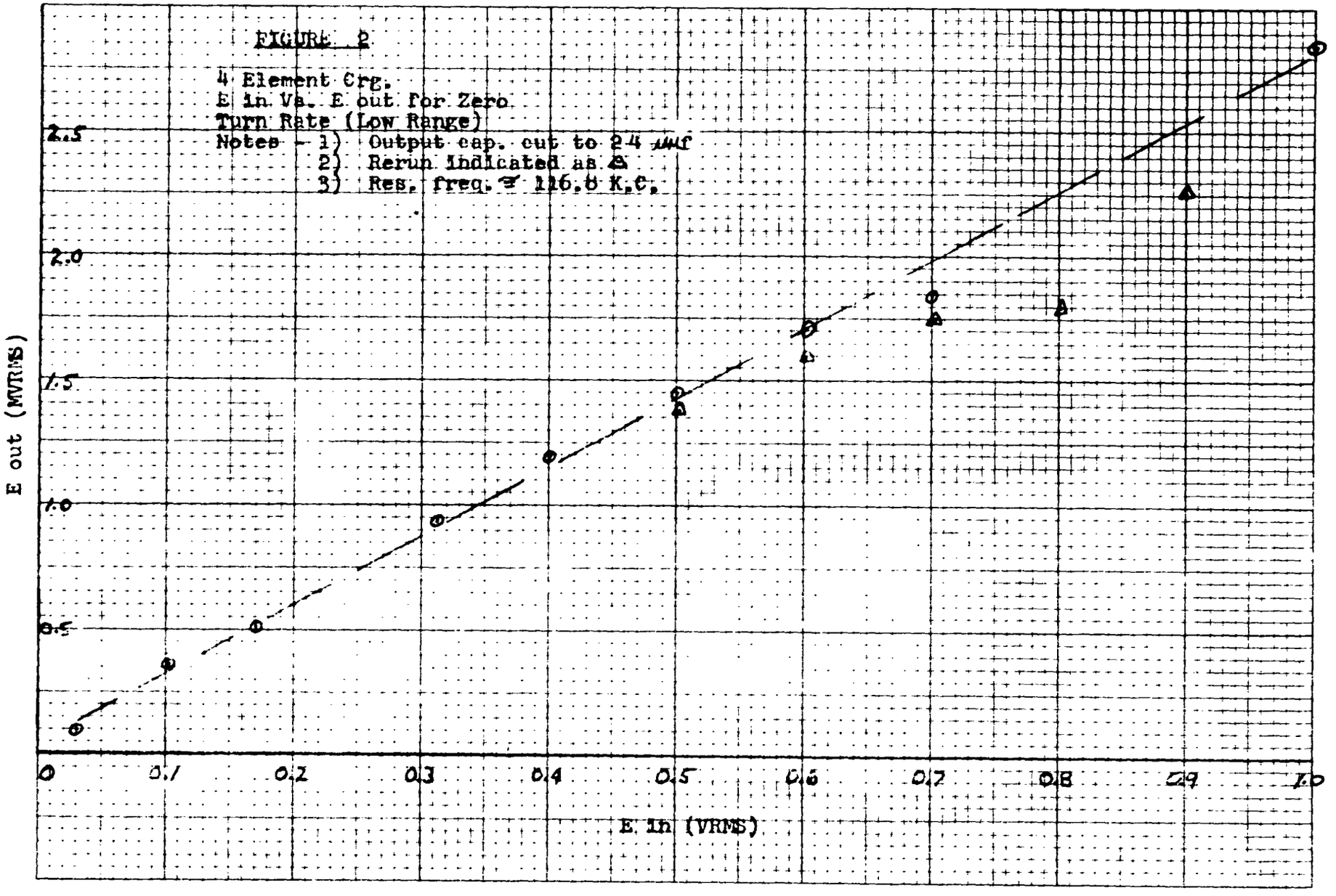

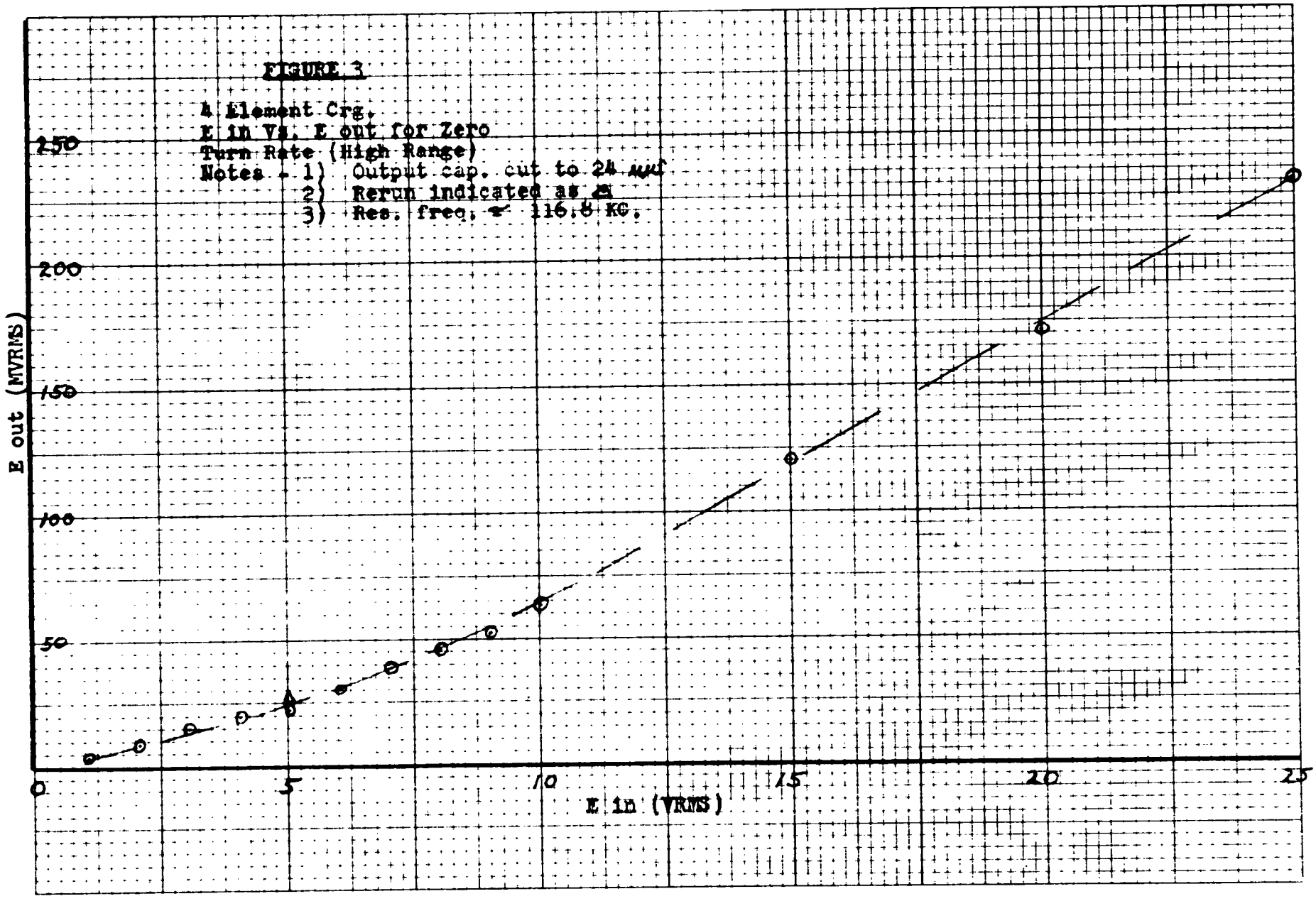

FIGURE 9a

PICKUP ELEMENT, PIN WHEEL GYRO, ON TURNTABLE

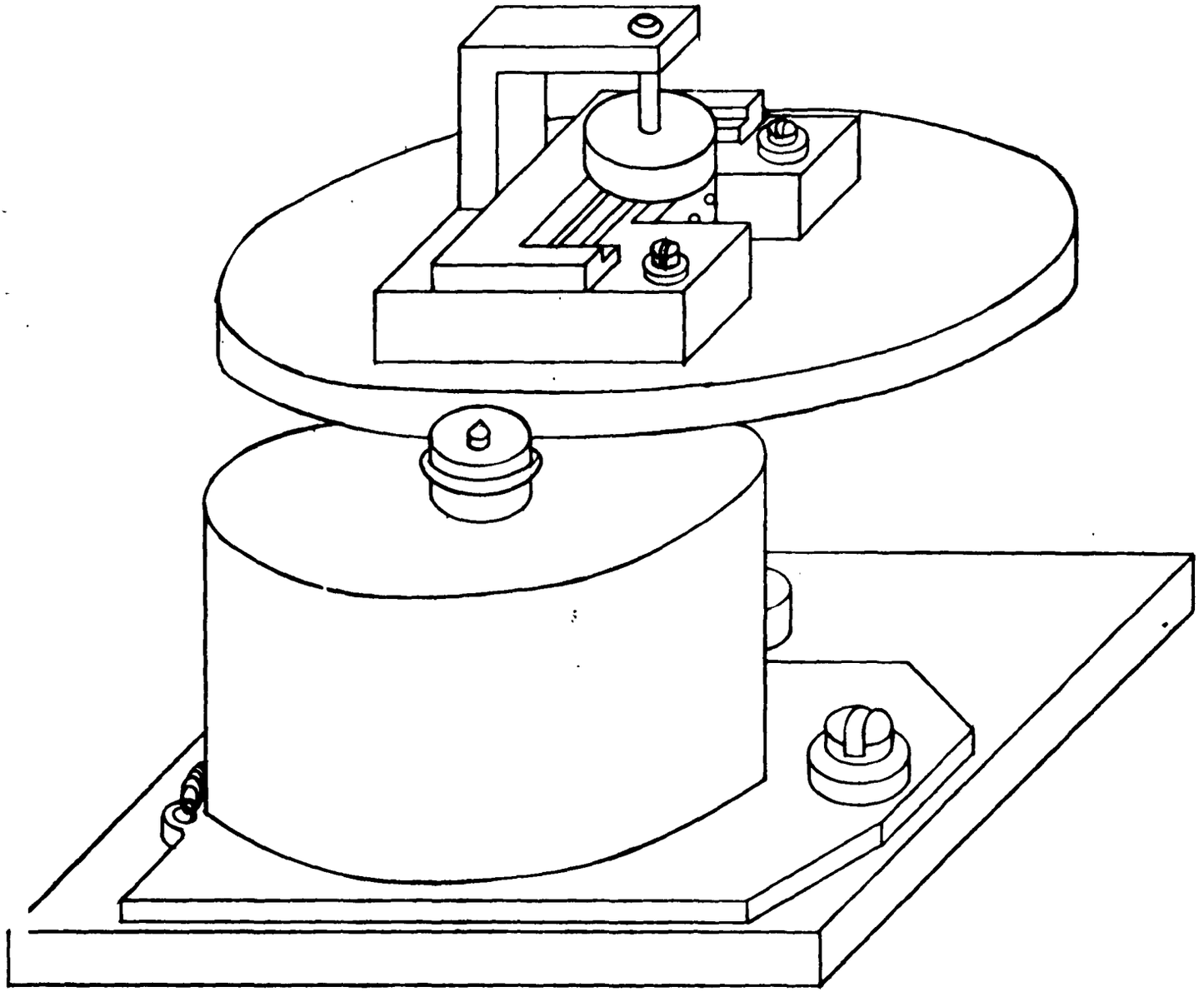

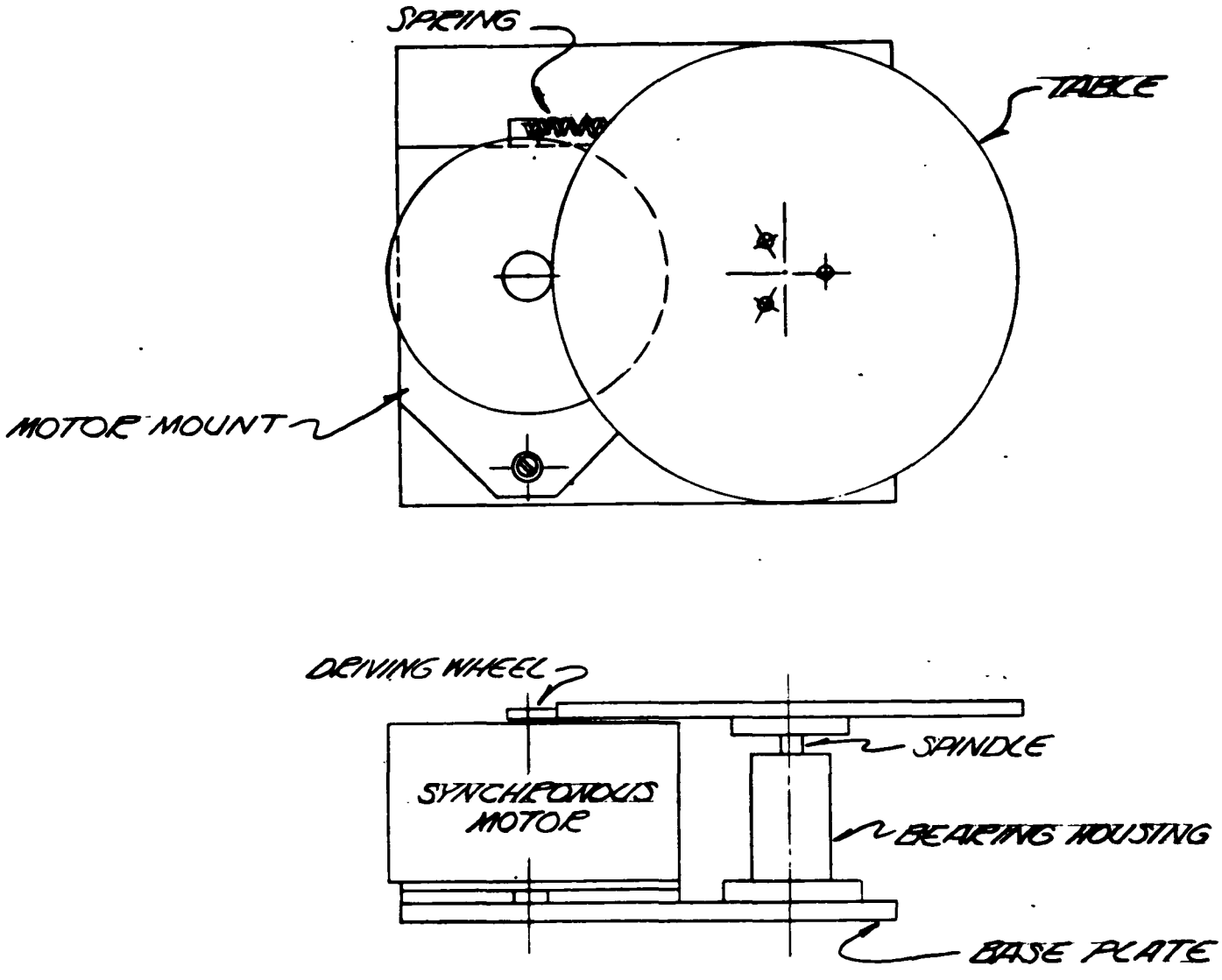

TURNTABLE (ASSEMBLY DWG) FIGURE 46

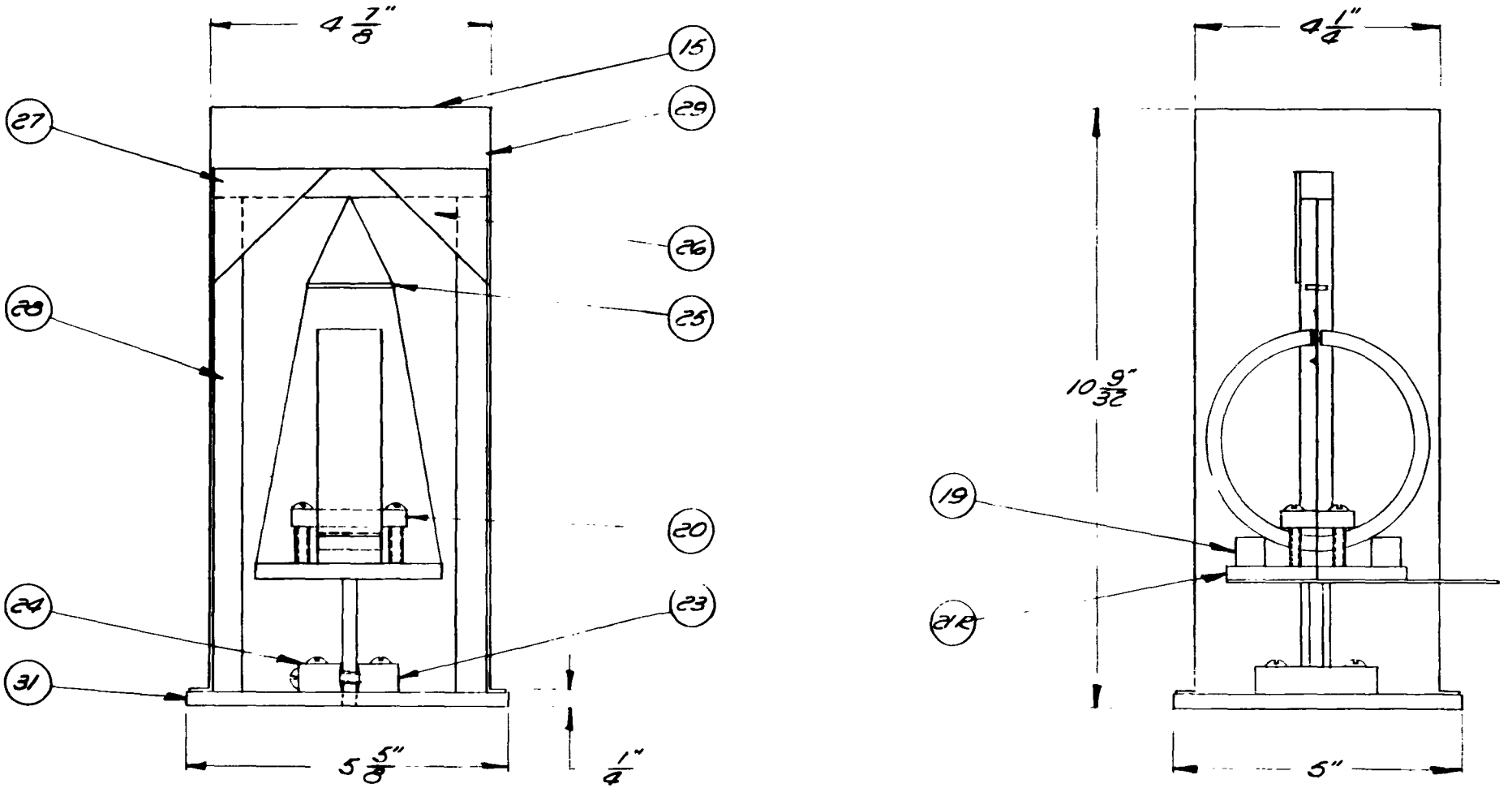

FIGURE 5
U3417 SPLIT CYLINDER ASS'Y
DWG C - ASS'Y SCALE 1/2

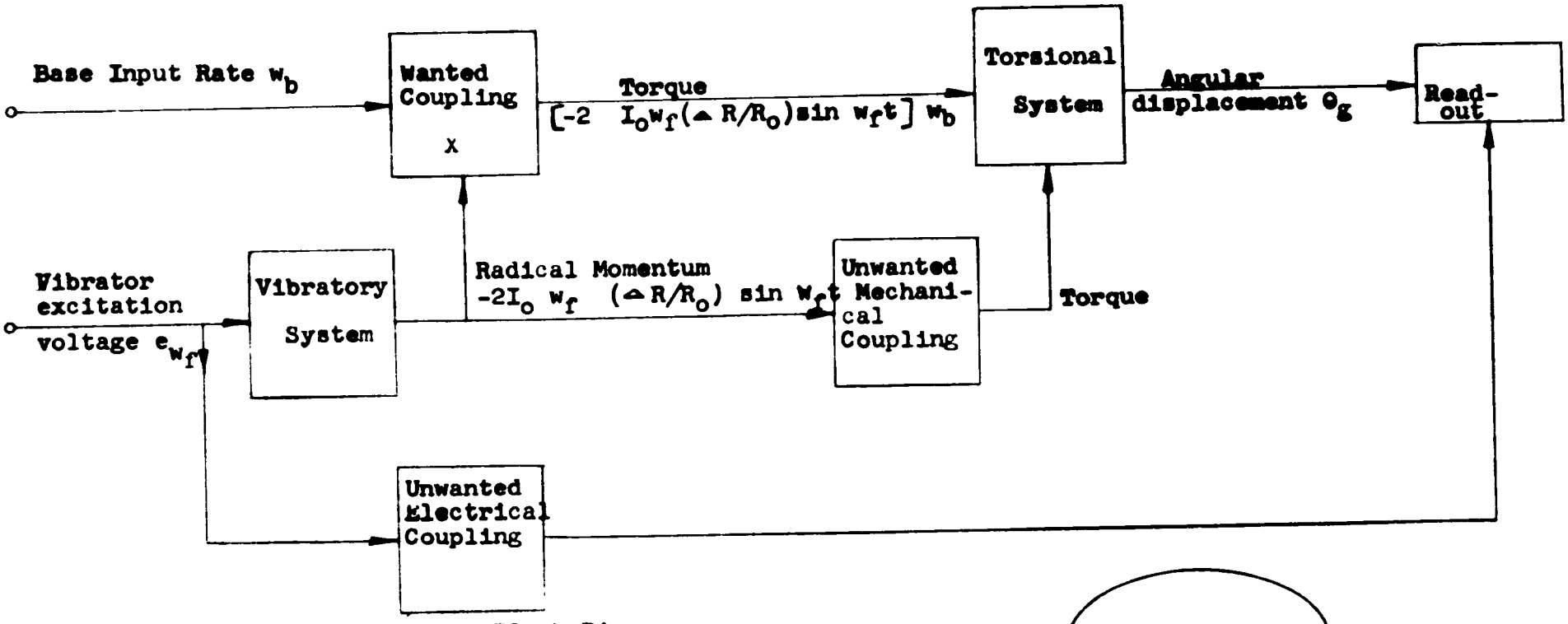

b. Block Diagram

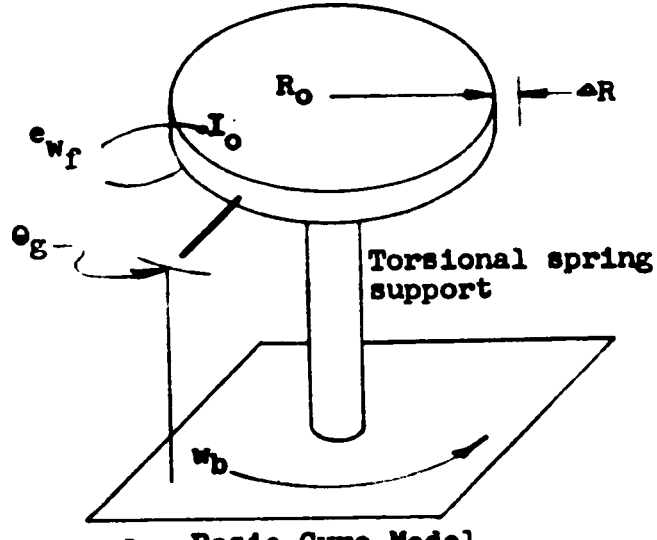

a. Basic Gyro Model

Figure 6. Rate Gyro

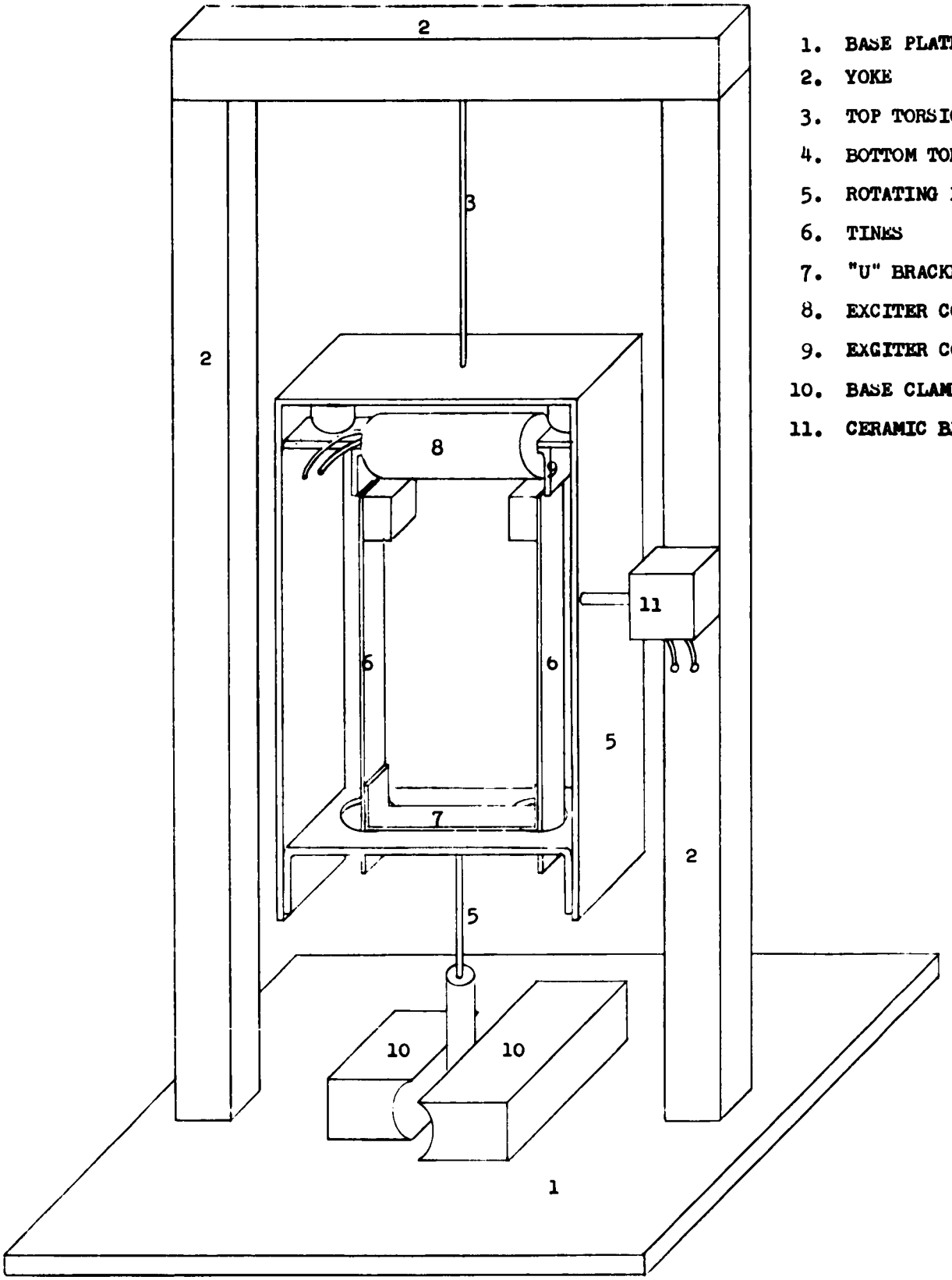

1. BASE PLATE
2. YOKE
3. TOP TORSION ROD
4. BOTTOM TORSION ROD
5. ROTATING FRAME
6. TINES
7. "U" BRACKET
8. EXCITER COIL
9. EXCITER CORE
10. BASE CLAMP
11. CERAMIC BENDER PICKUP

Figure 7 - Mechanical Tuning Fork

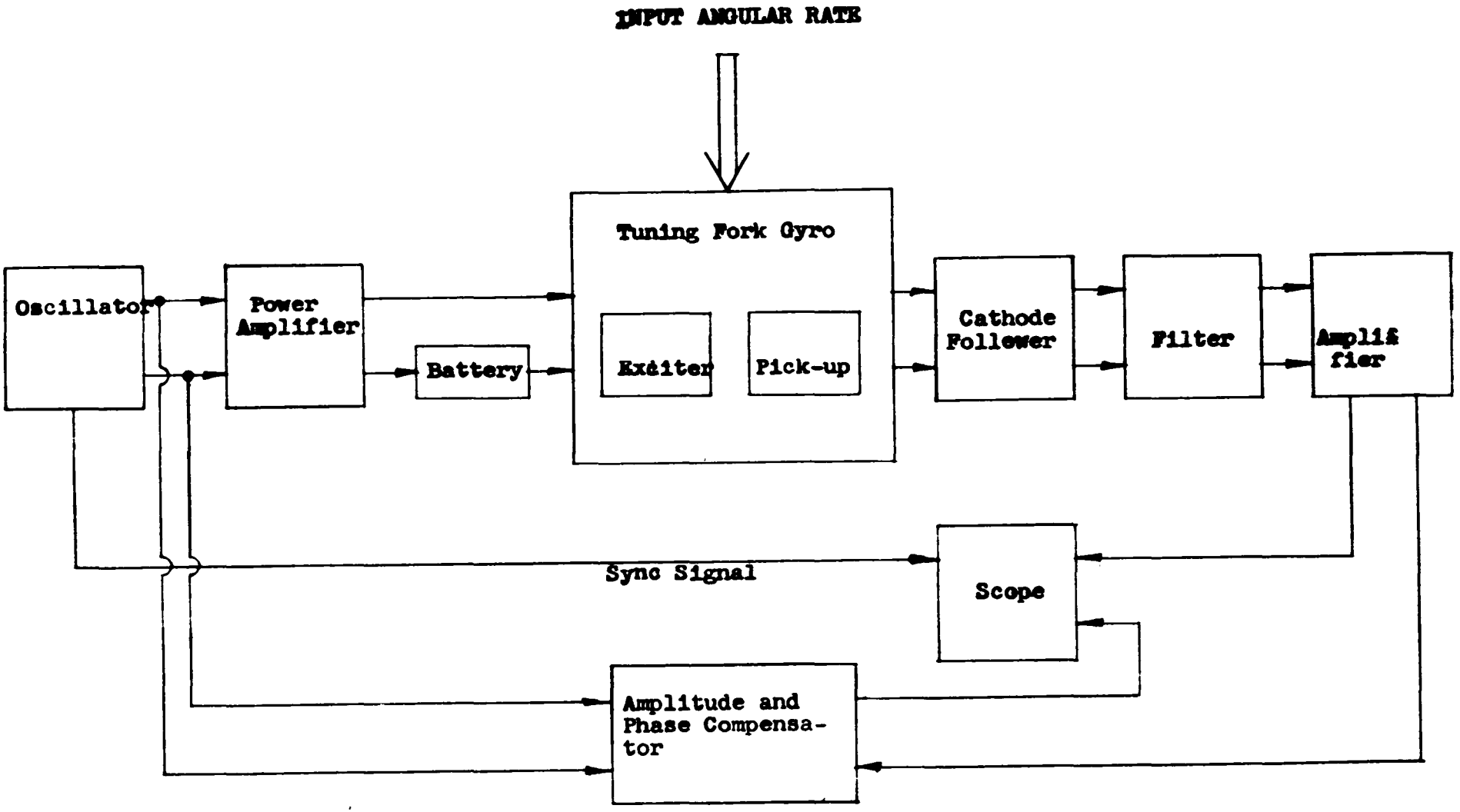

FIGURE 8

BLOCK DIAGRAM OF TUNING FORM GYRO TEST SETUP

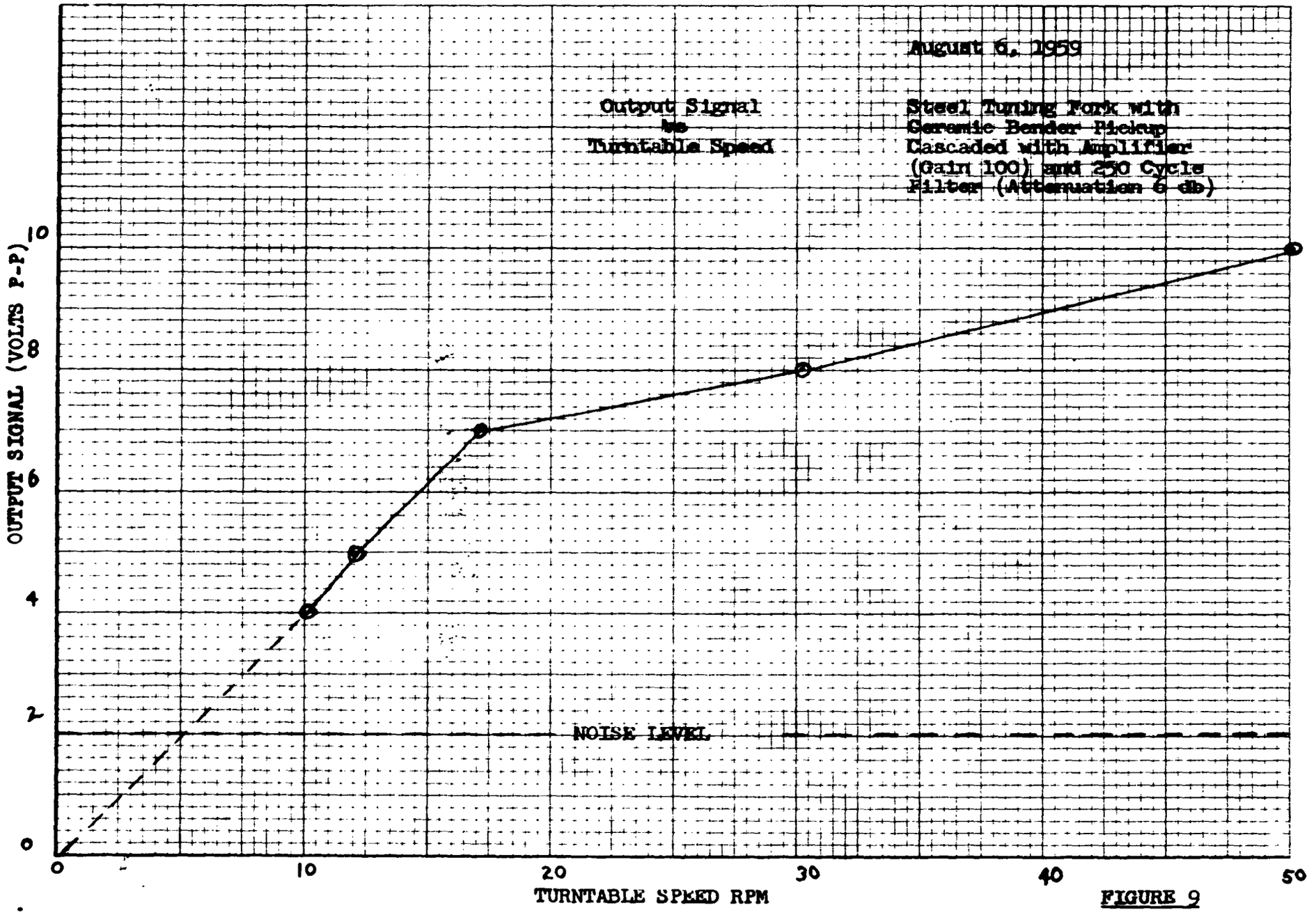

FIGURE 9

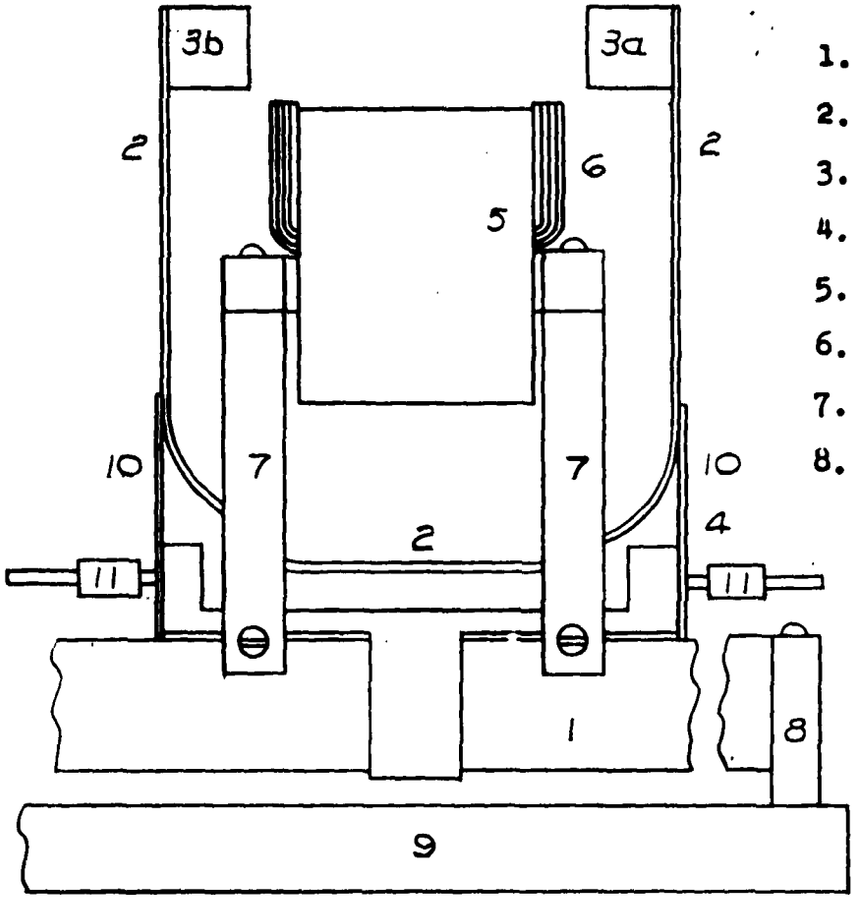

1. Leaf Spring
2. Leaf Spring
3. Soft Iron Weight
4. Soft Steel Bar
5. Coil
6. Core Lamination
7. Coil Support
8. Torsional Spring Mount (one on each side)
9. Base Plate
10. Tuning Fork Isolation Mount
11. Torsional Balance Weights (for adjusting torsional resonance)

MECHANICAL TUNING FORK II

FIGURE 10

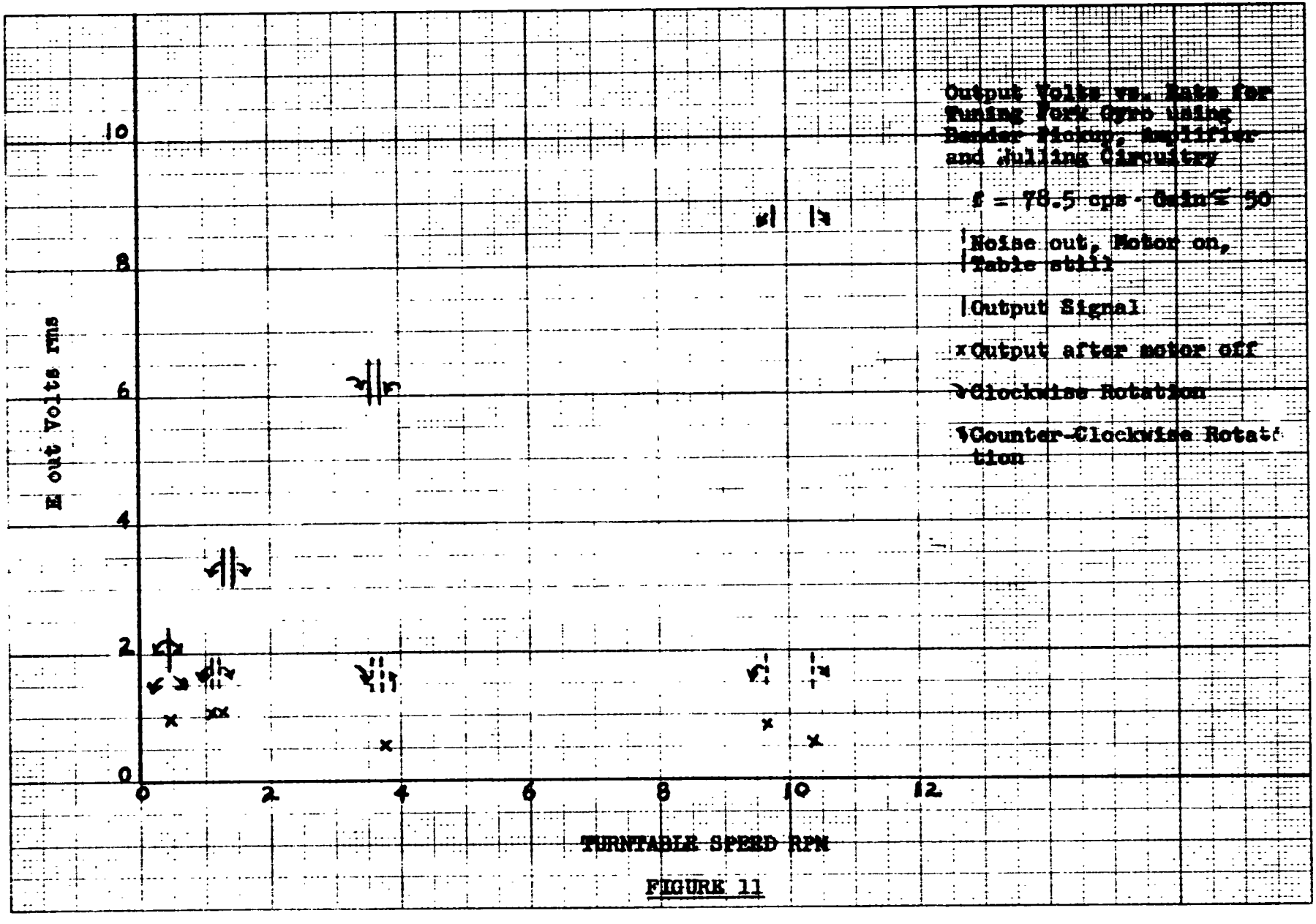

FIGURE 11

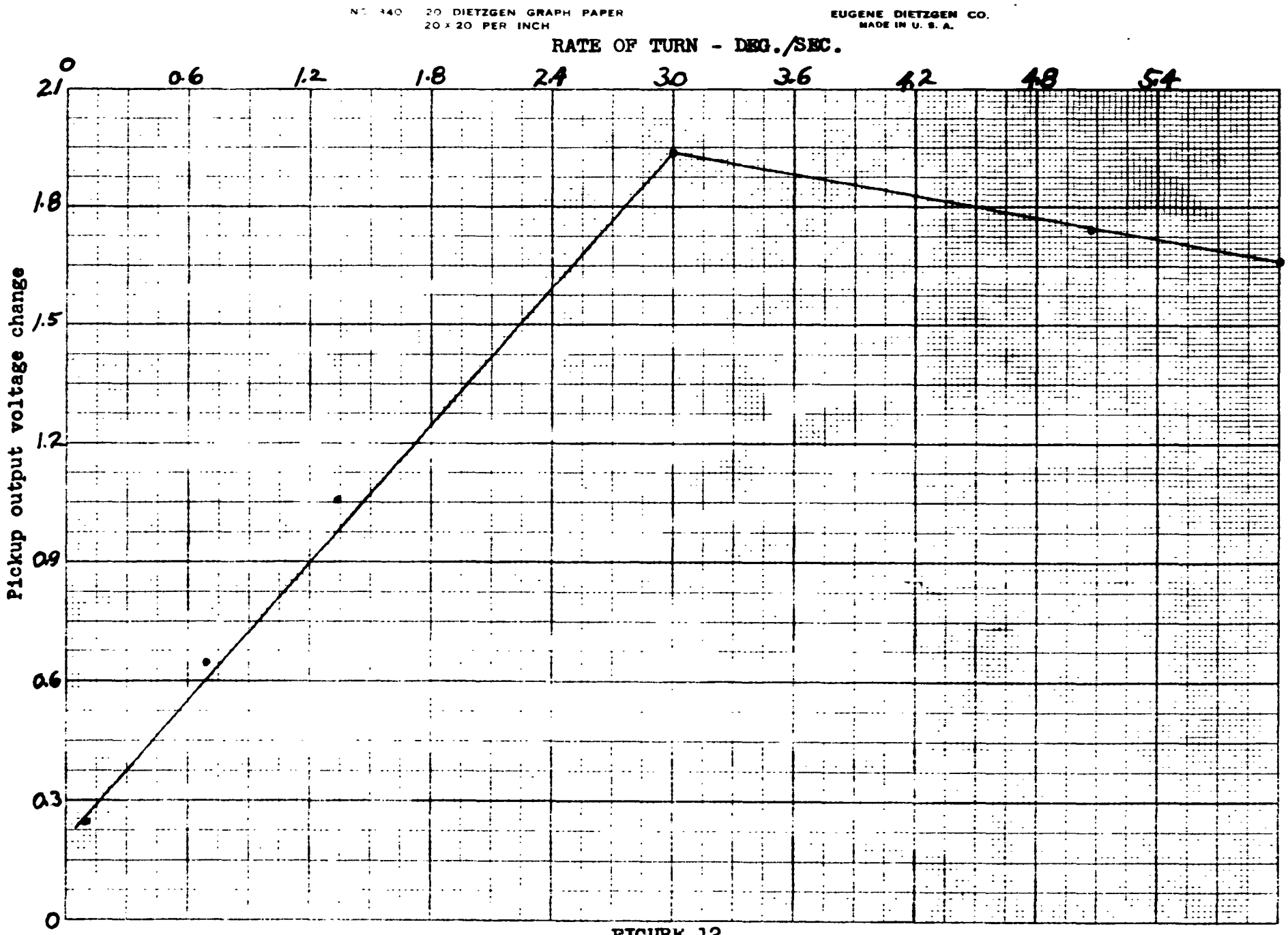
NO. 340 20 DIETZGEN GRAPH PAPER
20 x 20 PER INCH
EUGENE DIETZGEN CO.
MADE IN U. S. A.
RATE OF TURN - DEG./SEC.
0
0.6
1.2
1.8
2.4
3.0
3.6
4.2
4.8
5.4
Pickup output voltage change
2.1
1.8
1.5
1.2
0.9
0.6
0.3
0

FIGURE 12

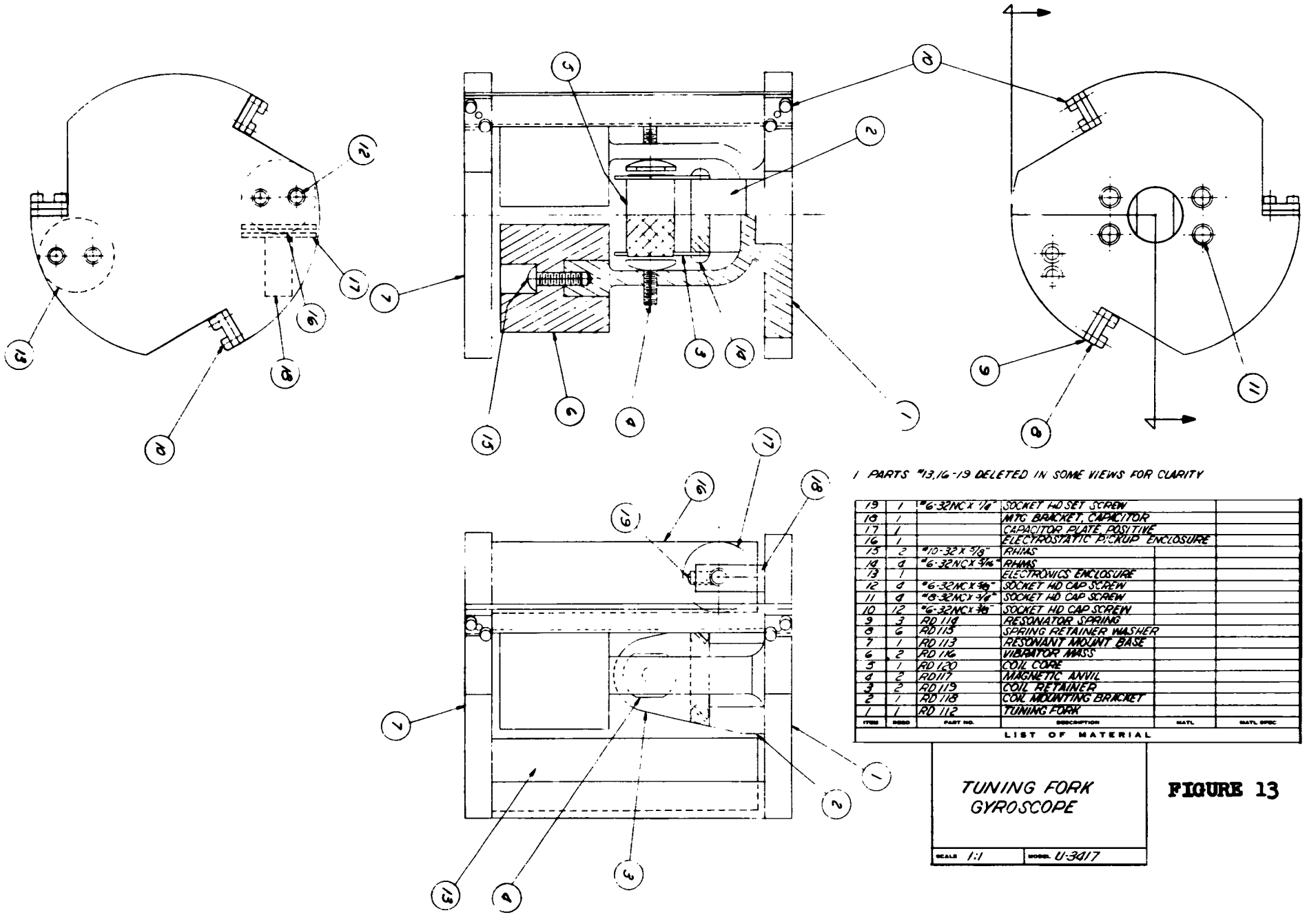

1 PARTS #13,16-19 DELETED IN SOME VIEWS FOR CLARITY

ITEM	REQD	PART NO.	DESCRIPTION	MATL	MATL SPEC
19	1	#6-32NC X 1/4"	SOCKET HD SET SCREW		
18	1		MTG BRACKET, CAPACITOR		
17	1		CAPACITOR PLATE, POSITIVE		
16	1		ELECTROSTATIC PICKUP ENCLOSURE		
15	2	#10-32 X 5/8"	RHMS		
14	4	#6-32NC X 3/16"	RHMS		
13	1		ELECTRONICS ENCLOSURE		
12	4	#6-32NC X 3/8"	SOCKET HD CAP SCREW		
11	4	#8-32NC X 3/4"	SOCKET HD CAP SCREW		
10	12	#6-32NC X 3/8"	SOCKET HD CAP SCREW		
9	3	RD 114	RESONATOR SPRING		
8	6	RD 113	SPRING RETAINER WASHER		
7	1	RD 113	RESONANT MOUNT BASE		
6	2	RD 116	VIBRATOR MASS		
5	1	RD 120	COIL CORE		
4	2	RD117	MAGNETIC ANVIL		
3	2	RD 119	COIL RETAINER		
2	1	RD 118	COIL MOUNTING BRACKET		
1	1	RD 112	TUNING FORK		

LIST OF MATERIAL

TUNING FORK GYROSCOPE

SCALE 1:1 | MODEL U-3017

FIGURE 13

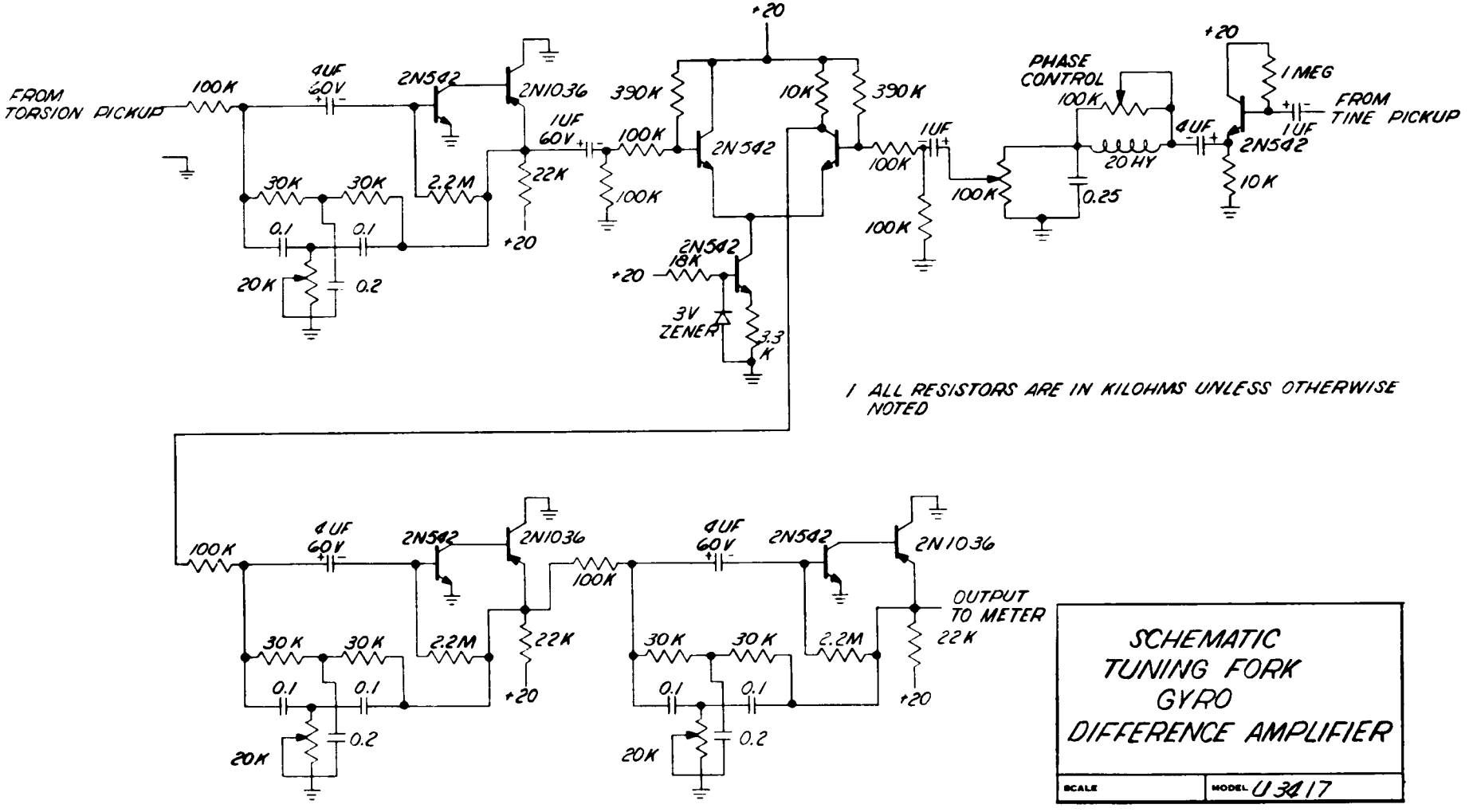

1 ALL RESISTORS ARE IN KILOHMS UNLESS OTHERWISE NOTED

SCHEMATIC
TUNING FORK
GYRO
DIFFERENCE AMPLIFIER

SCALE | MODEL U3417

FIGURE 14

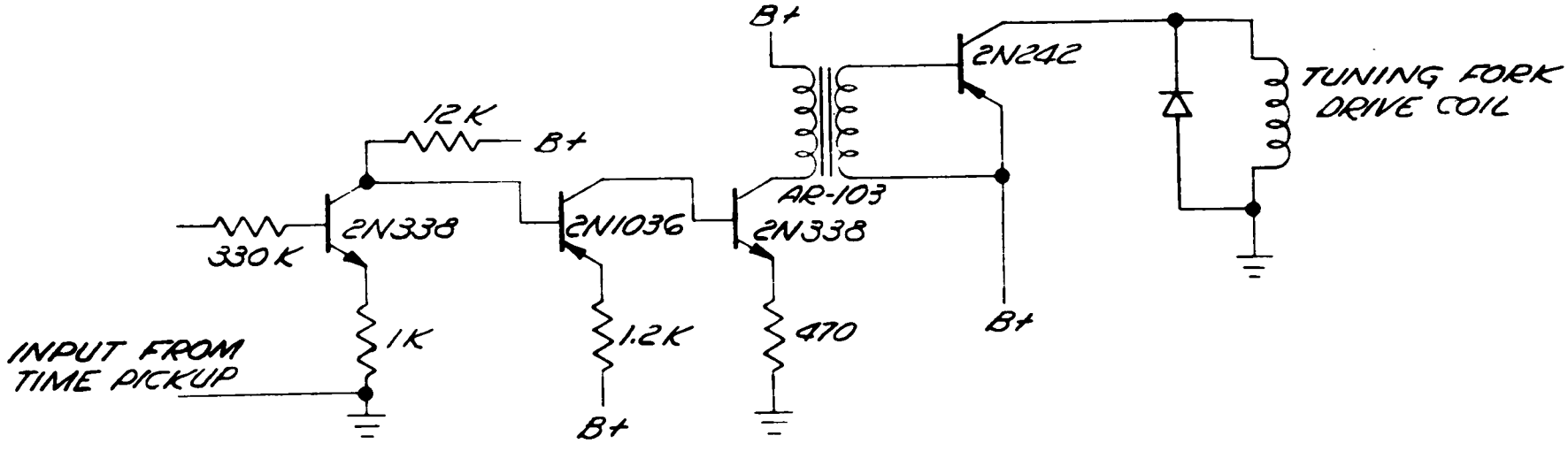

TUNING FORK DRIVE AMPLIFIER

Figure 15

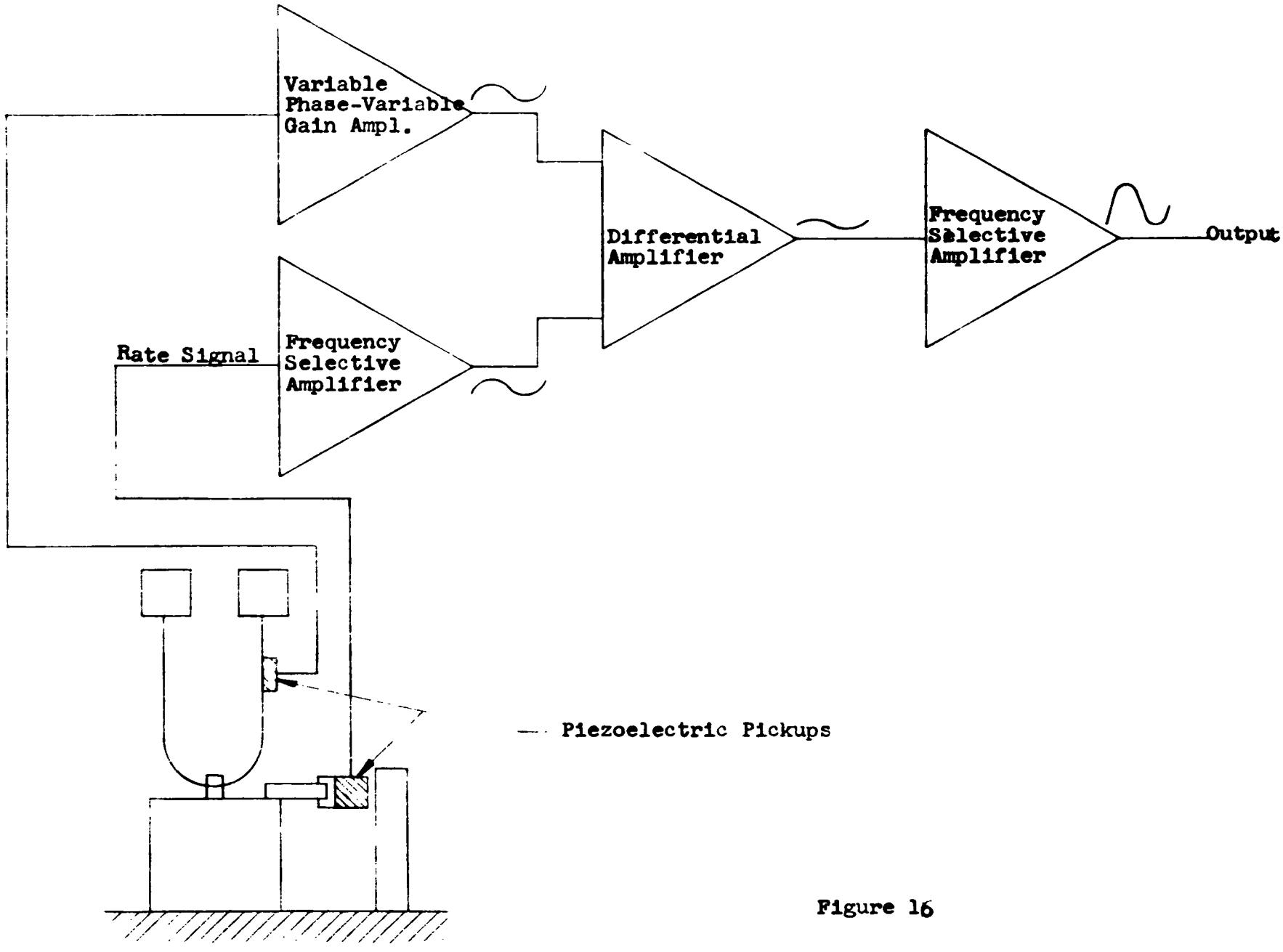
Variable
Phase-Variable
Gain Ampl.
Differential
Amplifier
Frequency
Selective
Amplifier
Output
Rate Signal
Frequency
Selective
Amplifier
— Piezoelectric Pickups

Figure 16

Figure 17

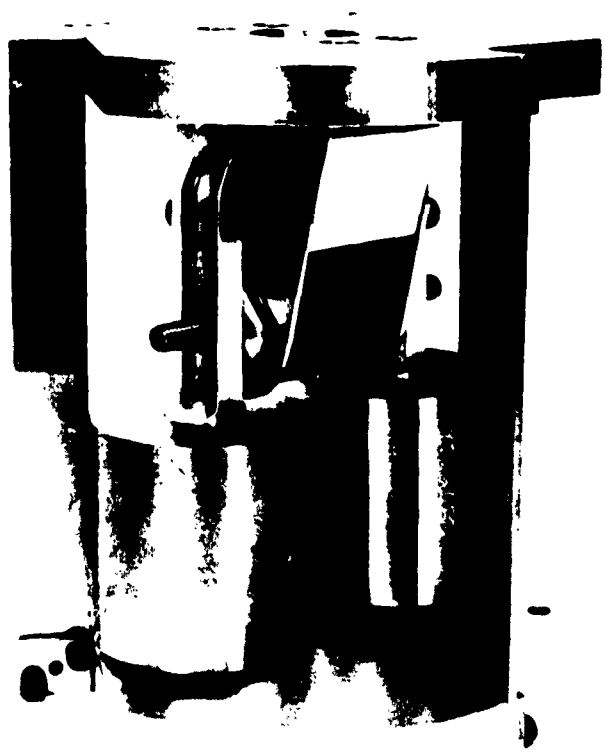

Figure 18